Université de Sherbrooke

CALCIUM CONTENT REGULATION IN SKELETAL AND CARDIAC MUSCLE IN PHYSIOLOGICAL CONDITIONS

by

Sandra Lopez Romero

Department of Pharmacology and Physiology

Thesis submitted at the Faculty of Medicine and Health Sciences in partial fulfillment of the degree of Master in Physiology

Sherbrooke, Québec, Canada

April 2018

Members of the jury

Dr Paul Pape Department of Pharmacology - Physiology
Dr Robert Dumaine Department of Pharmacology - Physiology
Dr Guylain Boulai Department of Pharmacology - Physiology

ABSTRACT

CALCIUM CONTENT REGULATION IN SKELETAL AND CARDIAC MUSCLE IN PHYSIOLOGICAL CONDITIONS

Sandra Lopez Romero

Department of Pharmacology and Physiology.

Thesis submitted at the Faculty of Medicine and Health Sciences in partial fulfillment of the degree of Master in Physiology. Faculty of Medicine and Health Sciences, Université de Sherbrooke, Sherbrooke, Québec, Canada, J1H 5N4

Calcium is an essential element involved in various physiological processes such as cell apoptosis and muscle contraction. Several pathologies have been associated to a bad intracellular Ca^{2+} handling, which leads to changes in total Ca^{2+} concentration in the muscle ($[Ca_T]_{WM}$). A new method has recently been developed in our laboratory (Lamboley et *al.*, 2015; J. Gen. Physiol., 145(2):127153) to measure $[Ca_T]_{WM}$ in skeletal and cardiac muscle, which allowed us to make the following observations: 1) $[Ca_T]_{WM}$ in mouse *extensor digitorum longus* (EDL), increases as the mouse weight / muscle weight ratio increases; 2) $[Ca_T]_{WM}$ in the EDL (but not in the soleus) and in the left ventricle of agitated/active mice was almost twofold higher than that of control mice. We hypothesize that there is one or multiple physiological mechanisms regulating $[Ca_T]_{WM}$ in the muscle to satisfy force requirements. Our goals are to find a group of reproductible conditions involved in $[Ca_T]_{WM}$ regulation, as well as adapting the previously mentioned method, so faster measurements can be performed. 36 mice were randomly assigned to one of the following groups: 1) control mice (rested); 2) injected with epinephrine or saline; 3) trained in a treadmill; 4) injected with epinephrine or saline and trained in a treadmill. $[Ca_T]_{Heart}$ values of control mice were ~27 times higher than those reported by other authors. Our results indicate a decrease in $[Ca_T]_{WM}$ in all the muscles studied in those mice under epinephrine, probably because of α-adrenergic stimulation dominating over β-adrenergic stimulation. This decrease was more pronounced when the treadmill training was added to the injection, probably because more Ca^{2+} is being released from the SR, so more Ca^{2+} can be extruded to the extracellular space. We report an increase of $[Ca_T]_{WM}$ in the EDL when the treadmill training is applied alone, which might represent a Ca^{2+} upregulation mechanism by which the muscle builds up intracellular Ca^{2+} to satisfy force requirements. The channels responsible for Ca^{2+} entry are yet to be identified. Finally, the adaptations applied on the technique proved to be useful for performing faster measurements.

Key words: calcium content, heart muscle, skeletal muscle, exercise, epinephrine.

RÉSUMÉ

RÉGULATION DE LA TENEUR EN Ca^{2+} DU MUSCLE SQUELETTIQUE ET DU MUSCLE CARDIAQUE EN CONDITIONS PHYSIOLOGIQUES

Par Sandra Lopez Romero, département de Pharmacologie et Physiologie
Mémoire présentée à la Faculté de Médecine et des sciences de la santé en vue de l'obtention du diplôme de Maitrise en Physiologie. Faculté de médecine et des sciences de la santé, Université de Sherbrooke, Sherbrooke, Québec, Canada, J1H 5N4

Le Ca^{2+} est un élément se trouvant dans plusieurs processus physiologiques, parmi lesquels, la contraction musculaire et l'apoptose cellulaire. Plusieurs pathologies sont associées à une mauvaise régulation du Ca^{2+} intracellulaire. Une nouvelle méthode a été développée dans notre laboratoire (Lamboley et *al.*, 2015; J. Gen. Physiol., 145(2):127153), afin de mesurer la concentration totale de Ca^{2+} dans le muscle ($[Ca_T]_{WM}$) de souris, ce qui nous a permis de faire les observations suivantes : 1) Pour *l'extensor digitorum longus* (EDL), plus le ratio poids de l'EDL/poids de la souris augmente, plus la $[Ca_T]_{WM}$ est élevée et 2) la $[Ca_T]_{WM}$ dans l'EDL (mais pas dans le soléaire) et dans le ventricule gauche des souris agitées/actives était environ 2 fois plus élevée que celle des souris témoins. Notre hypothèse est qu'il existe un ou plusieurs mécanismes qui régulent la $[Ca_T]_{WM}$ du muscle pour répondre à une demande spécifique de force. Nos buts sont de trouver un ensemble de conditions reproductibles affectant la $[Ca_T]_{WM}$, ainsi que d'adapter la méthode utilisée afin de la rendre plus efficace. 36 souris ont été distribuées aléatoirement en plusieurs groupes : 1) souris témoins; 2) injectées à l'épinéphrine ou au salin; 3) injectées à l'épinéphrine ou avec une solution saline et entrainées avec un tapis roulant. La $[Ca_T]_{Cardiaque}$ mesurée a été ~27 fois plus élevée que celle rapportée par d'autres auteurs. Nos résultats indiquent une diminution de la $[Ca_T]_{WM}$ dans tous les muscles étudiés dans le cas des souris injectées a l'épinéphrine, peut-être dû à la dominance de la stimulation α-adrénergique sur la stimulation β-adrénergique. Cette diminution a été plus prononcée quand l'entrainement dans le tapis roulant a été combiné avec l'injection, puisque plus de Ca^{2+} est relâché à partir du RS, donc plus de Ca^{2+} peut être extrudé au milieu extracellulaire. Nous avons aussi observé une augmentation de la $[Ca_T]_{WM}$ dans l'EDL, quand seul l'entrainement a été appliqué, ce qui pourrait représenter le mécanisme de régulation que nous cherchons. Par contre, les canaux impliqués n'ont pas encore été identifiés. Finalement, les adaptations appliquées sur la méthode nous ont permis de réaliser des mesures de Ca^{2+} plus rapidement.

Mots clés: teneur en calcium, muscle cardiaque, muscle squelettique, exercice, adrénaline.

TABLE OF CONTENTS

LIST OF ILLUSTRATIONS

LIST OF TABLES

LIST OF ABBREVIATIONS AND SYMBOLS

0Ca/0Na	Calcium-free / Sodium-free
AAS	Atomic absorbance spectroscopy
ACh	Acetylcholine
ADP	Adenosine diphosphate
AP	Action potential
ATP	Adenosine triphosphate
BAPTA	1,2-Bis(2-aminophenoxy) ethane-N,N,N′,N′-tetraacetic acid tetrakis
BCP	Biceps
BR	*Brachioradialis*
Ca^{2+}	Free calcium
$Ca_{background}$	Calcium coming from sources other than the muscle sample
$CaCl_2$	Calcium chloride
CaM	Calmodulin
CaMKII	Calmodulin kinase II
Ca-BAPTA	Calcium bound to BAPTA
CFPA-FMSS	Comité facultaire de protection des animaux de la Faculté de médicine et des sciences de la santé
CholineCl	Choline chloride
CICR	Calcium-induced calcium release
CON	Control group
DHPR	Dihydropyridine receptor
DMD	Duchenne muscle dystrophy
E-C coupling	Excitation – contraction coupling
EDL	*Extensor digitorum longus*
EGTA	Ethylene glycol-bis(2-aminoethylether)-N,N,N′,N′-tetraacetic acid
EPI	Group of mice injected with epinephrine
EPI+Ex	Group of mice injected with epinephrine and exercised in a treadmill
Ex	Exercise group
HEPES	4-(2-hydroxyethyl)-1-piperazineethanesulfonic acid)
HF	Heart failure
KCl	Potassium chloride
LTCC	L (long lasting) – type calcium channels
Mg^{2+}	Magnesium
$MgCl_2$	Magnesium chloride
MS	Measurement solution
Na^{+}	Sodium
NaCl	Sodium chloride
NaOH	Sodium hydroxy
NCX	Sodium – calcium exchanger
P_i	Inorganic phosphate
PKA	Protein kinase A
PLB	Phospholamban
RyR_1	Type 1 ryanodine receptors
RyR_2	Type 2 ryanodine receptors
SAL	Saline group
SAL+Ex	Saline combined with exercise group

SDS	Sodium dodecyl sulfate
SERCA	Sarcoplasmic reticulum calcium ATPase
SLN	Sarcolipin
SACs	Stretch-activated calcium channels
SOCs	Store-operated calcium channels
Sol	Soleus
SR	Sarcoplasmic reticulum
TnC	Troponin C
T-tubules	Transversal tubules
$[Ca^{2+}]$	Free calcium concentration
$[Ca^{2+}]i$	Intracellular calcium concentration
$[Ca_T]$	Total calcium concentration
$[Ca_T]_{WM}$	Total calcium concentration in the whole muscle

ACKNOWLEDGEMENTS

This project was financed by the NSERC and was fully developed in the Université de Sherbrooke.

While not part of this thesis, I want to thank Robert Dumaine (Université de Sherbrooke) for the chance to do a rotation in his lab.

Special thanks to Eric Rousseau (Université de Sherbrooke), for his useful advice, Jean-Bernard Denault (Université de Sherbrooke), who allowed me to use the plate reader, Abby McDonell (Queen's University), who worked in the preliminary data collection and Fatou Touré (Université de Sherbrooke) who has also been involved in the development of the technique used in this study. Finally, I am especially grateful to my supervisor, Paul Pape (Université de Sherbrooke), whose help, patience, attitude and disposition made this work possible.

INTRODUCTION

1. Muscle anatomy

The body contains three types of muscle tissue: skeletal, cardiac and smooth muscle. This thesis focuses on the first two types.

1.1 Skeletal muscle

The skeletal muscle includes not only skeletal muscle fibers (which will be properly introduced later in this section), but also blood vessels, lymphatic vessels, nerve fibers and connective tissue, which provides structure to the muscle and compartmentalizes the muscle cells (Tortora & Derrickson, 2012). Skeletal muscles are often connected to the bones by tendons, which are extensions of the connective tissue that conduct the tension generated by the muscles to the bones. In other cases, muscles might be bound to bones by aponeurosis, a tendon-like sheet also a result of the extension of the connective tissue.

The most important structures of muscle tissue are muscle cells, also called muscle fibers (Fig. 1). Inside each skeletal muscle, muscle fibers are organized in fascicles separated by connective tissue (particularly collagen and reticular fibers) (Betts *et al*., 2013). The plasma membrane (known as sarcolemma) of a muscle fiber displays a series of invaginations called transverse (T) tubules filled with interstitial fluid (Tortora & Derrickson, 2012). The sarcolemma surrounds the cytoplasm of the muscle cell, also referred to as the sarcoplasm, that contains small striated structures called myofibrils that are composed by protein structures called myofilaments (Betts *et al*., 2013). The myofilaments are classified as thick or thin myofilaments. The main component of the thick filaments is myosin, which works as the motor protein in all types of muscle by using energy coming from ATP. In the case of the thin filaments the main component is the protein actin, that is equipped with myosin – binding sites, although two essential regulatory proteins can be also found: tropomyosin and troponin. The thick and thin filament are arranged in compartments called sarcomeres (Fig. 2), the functional units of myofibrils, delimited by regions with high protein content called Z discs. Since the filaments do not extend the entire length of the muscle fiber, the sarcomere contains zones with only one type of filaments, as well as zones where the two types of filaments overlap. The Z discs are located in the middle of the I bands, which are zones

containing only thin filaments, a fact that gives them a lighter color. Moving from the extremes towards the middle of the sarcomere, the thick and thin filaments overlap forming the A band, a much darker zone that represents the length of the thick filaments. In the center of the sarcomere, within the A bands, there is a smaller zone with only thick filaments, called the H zone. In the middle of the sarcomere, surrounded by the H zone and the A bands, supporting proteins that hold the thick filaments together form the M line, which represents the middle of the sarcomere (Tortora & Derrickson, 2012).

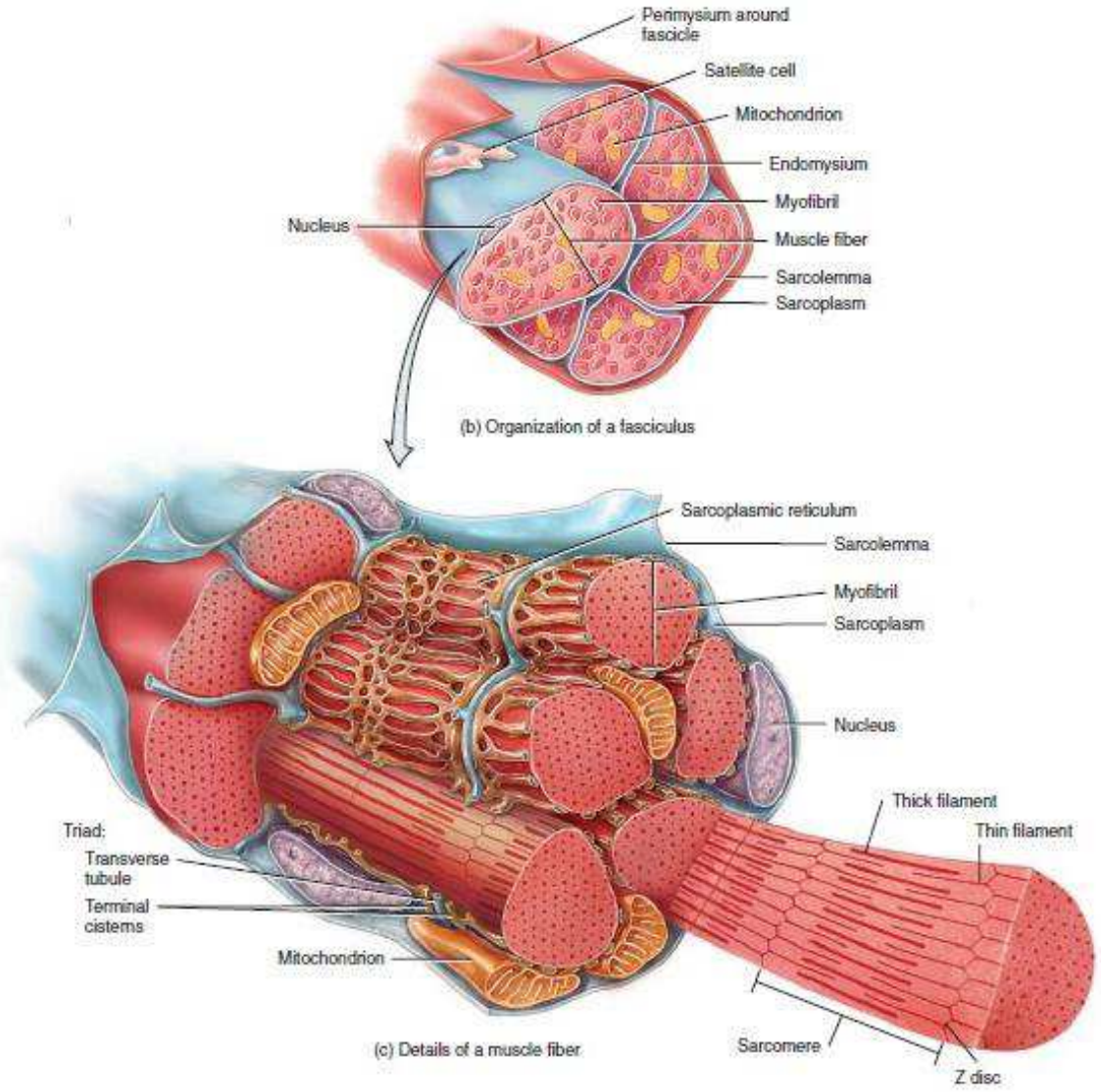

Figure 1. Organization of skeletal muscle. Fig. 1A shows the organization of muscle cells in fascicles. Muscle fibers are organized in fascicles separated by connective tissue (particularly collagen and reticular fibers). Fig. 1B shows a detail of a muscle fiber. The sarcolemma displays a series of invaginations called transverse tubules and it surrounds the sarcoplasm of the muscle cell which contains the myofibrils. The myofilaments of the myofibrils are also shown. Image corresponding to Fig. 10.2 in Tortora & Derrickson, 2012.

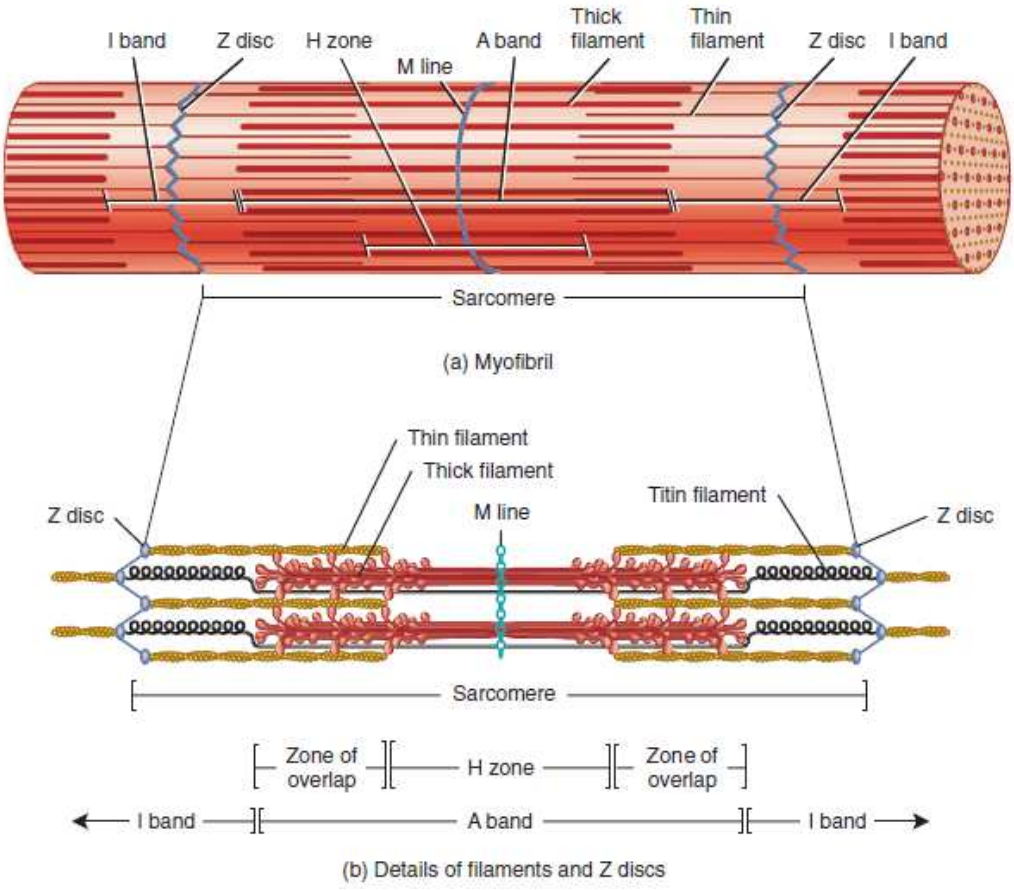

Figure 2. Organization of myofilaments in a myofibril. Fig. 2A shows the disposition of the thin and thick filaments in a myofibril and the different zones this disposition allows to differentiate. Fig.2B shows the same, only the filaments are more detailed. Image corresponding to Fig. 10.3 in Tortora & Derrickson, 2012.

Among the organelles present in a muscle cell, an especially important one is a fluid-filled system of membranous sacs called the sarcoplasmic reticulum (SR) (Tortora & Derrickson, 2012). The SR is a specialized smooth endoplasmic reticulum which stores, releases and retrieves calcium (Betts *et al*., 2013). The Ca^{2+} fluxes across the SR membrane are primarily controlled by the type 1 ryanodine receptors (RyR_1) and the SR Ca^{2+} ATPase (SERCA pump). The RyR_1s are calcium channels located in the membrane of the SR that regulate the calcium outflow towards the cytoplasm (Calderon, 2014) and their open probability is increased by sarcoplasmic [Ca^{2+}] among other factors (Diaz et al., 2005). Their activity is regulated by various proteins, such as FKBP12.6 (or calstabin 2), calmodulin (CaM), CaMKII, PKA and protein phosphatases 1 and 2 (Neef & Maier, 2013). The SERCA pump is a protein, also located on the SR membrane, that uses the energy derived from ATP hydrolysis to transport Ca^{2+} into the SR. RyR_1 are mechanically coupled to voltages sensors

called L-type calcium channels (LTCCs) or DHPRs (Franzini-Armstrong *et al*, 1994), transmembrane proteins/channels located in a region of the T-system called a triad. The triads are regions where one tubular element of the T-system is found between two terminal segments of SR (Porter and Palace, 1957).

The role of the LTCCs, the RyR_1 and the myofilaments in muscle contraction will be covered later.

1.2 Cardiac muscle

There are some differences between skeletal and cardiac muscle tissue. Although most of the heart is myocardium, there are also other types of tissue present that is important to take into consideration. The importance of a good histological knowledge of the heart for my project will become clearer later.

The heart is an organ composed of multiple layers (Fig. 3). Protecting the heart, so in the most external part, we find the pericardium, a membrane composed of two elements. From the outer to the inner part of the heart, we find in the first place the fibrous pericardium, a membrane mainly composed of connective tissue. The second element is the serous pericardium, that encompasses two thin membranes separated by serum or pericardial fluid: the parietal layer, fused to the fibrous pericardium and the visceral layer, composed of mesothelium. The visceral layer is also considered to belong to one of the layers of the heart wall. The heart wall consists of three layers, the most external one being the epicardium, composed of the already mentioned visceral layer and a second layer of variable composition, where the adipose tissue is the predominant element. Blood and lymphatic vessel are also present in this layer. Internal to the epicardium we find the myocardium, a layer of striated muscle. Cardiac muscle cells are similar to skeletal fibers, only shorter and less circular and they exhibit branching. Neighboring fibers connect by thickenings of the sarcolemma, the intercalated discs. Finally, inner to the myocardium, the endocardium, a layer of endothelium placed over a layer of connective tissue, can be found (Tortora & Derrickson, 2012). Other kinds of tissue can be also found in the heart, such as the Purkinje fibers, present in the heart ventricles, right below the endocardium.

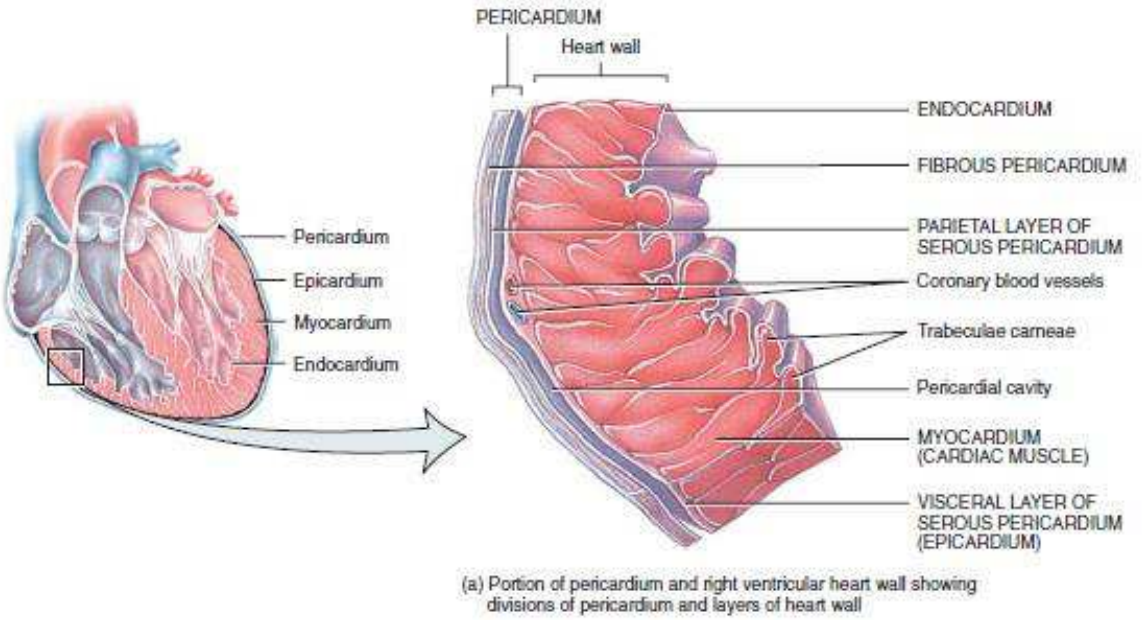

Figure 3. Portion of pericardium and the heart wall layers. The pericardium is the most external of the layers of the heart and it is composed of the fibrous pericardium and the serous pericardium. The serous pericardium is composed of the parietal layer and the visceral layer, which is also considered to be a part of the most external of the three layers of the heart wall, the epicardium. Inner to the epicardium, a layer of muscle tissue, the myocardium can be found. The innermost layer of the heart wall is the endocardium, a layer of endothelium placed over a thin layer of connective tissue. Partial image corresponding to Fig. 20.2 in Tortora & Derrickson, 2012.

Regarding internal components, there are also some differences among skeletal and cardiac muscle that are relevant for us. As in the skeletal muscle, in cardiac tissue, we find regions where the junctional SR makes close contact with the T-tubule membrane (Eisner *et al.*, 2017). These regions are called dyads. However, in the heart, it is the inward influx of Ca^{2+} through LTCC which triggers the opening of the type 2 ryanodine receptors (RyR_2) (Protasi, 2002), as explained in next sections. The SERCA pump is also present in cardiac muscle and its activity is primarily regulated by the protein phospholamban (PLB) which, in a non-phosphorylated state, inhibits SERCA activity (Periasamy *et al.*, 2007).

The action potential generation and certain steps of the excitation – contraction coupling process in the heart also differ from those of the skeletal muscle. This will be discussed later in this section.

2. Excitation contraction coupling

The term “excitation-contraction (EC) coupling” refers to the sequence of events from electrical excitation of the myocyte to the contraction of the heart (Bers, 2002) or the skeletal muscle. In the case of the skeletal muscle, a neurotransmitter, acetylcholine (ACh), released into the motor plate by the inferior motor neuron acts as an initiator for the action potential (AP) in muscle fibers (Calderon *et al,* 2014). The ACh binds receptors located in the plasmatic membrane of the muscle cell and, as a result, they undergo a conformational change that open a pore. Positively charged ions can now pass through into the muscle cell, causing a membrane depolarization. Thanks to this depolarization another type of channel, the voltage – gated sodium channel, opens. Na^+ can now enter the muscle cell, bringing the membrane potential to positive values thereby triggering an action potential that propagates throughout the membrane and the T-tubules system (Betts *et al*., 2013). In the heart, APs are caused by a group of self-excitable muscle fibers that depolarized to the threshold. The AP starts in the sinoatrial node, where these autorhythmic cells are located, and propagates to the neighboring cells causing the opening of the voltage – gated Na channels, similar to the skeletal muscle. The arrival of the depolarization to a triad (in skeletal muscle) or a dyad (in the heart) causes a still unclear conformational change in the LTCC (Calderon *et al*, 2014), channels responsible for most of the calcium current across the sarcoplasm (Bers, 2002). As mentioned previously, in skeletal muscle the LTCC are in physical contact with the RyR_1 (Franzini – Armstrong *et al*, 1994) and they act as voltage sensors involved in the opening of the RyR_1, a process that can be monitored with a gating current termed intramembranous charge movement (Schneider & Chandler, 1973, Pape & Carrier, 2002). The most widely accepted coupling mechanism in cardiac muscle involves Ca^{2+} - induced Ca^{2+} - release (CICR) mediated by the LTCC current. According to this mechanism, 2 – 4 Ca^{2+} ions binding to a RyR_2 are enough to trigger Ca^{2+} release from the SR (Bers, 2002). In both cases (cardiac and skeletal muscle), the cytosolic [Ca^{2+}] increases due to Ca^{2+} release from the SR. The presence of Ca^{2+} in the sarcoplasm triggers muscle contraction. In a filament relaxation state, regulatory proteins prevent interaction of myosin and actin. The regulatory protein troponin is conformed of 3 subunits: troponin C (TnC), the Ca^{2+} binding component; troponin T, the tropomyosin binding subunit and troponin I the inhibitory subunit, so-called because it binds to actin and inhibits actomyosin ATPase activity (Grabarek *et al*, 1992). The Ca^{2+} released into the sarcoplasm from the SR binds TnC, which causes the tropomyosin to move away from the myosin-binding sites on actin. When this happens, the contraction cycle begins: ATP is hydrolyzed to ADP + P_i (that remains bound to the myosin)

thanks to the action of an ATPase located in the myosin “heads”. This leads to a reorientation of the myosin “heads”. The myosin “heads” attach, then, to the myosin-binding site on actin forming the so-called cross-bridges and the phosphate group is released. In the next step, the site on the cross-bridges where the ADP is still bound, opens. The cross-bridges rotate, and the ADP is released. This rotation causes the sliding of the thin filament past the thick filament, which shortens the length of the sarcomere. In the last step, another ATP comes to bind its binding site on the myosin causing the detachment of the myosin “heads” to the actin. (Tortora & Derrickson, 2012). As long as Ca^{2+} is present in the sarcoplasm, this so-called “cross-bridge cycle” keeps on working. Ca^{2+} must be removed from the sarcoplasm to allow relaxation. In the heart, this is mostly achieved by the closing of the RyR, the activity of the SERCA pump of the SR and the extrusion of Ca^{2+} towards the extracellular medium by the Na^{+}/Ca^{2+} exchanger (NCX) (Eisner *et al.*, 2017). The quantitative importance of SERCA pump and the NCX in calcium removal varies depending on the species (Bers, 2002).

3. Calcium and muscle contractility of cardiac tissue

As mentioned in the previous section, the presence of calcium in the sarcoplasm is crucial for muscle contraction. As shown in Fig 2 of Bers, 2002, there is a correlation between total calcium concentration in a cell (and, also, the free intracellular calcium concentration ($[Ca^{2+}]i$)) and the force of contraction of the heart, increasing the force of contraction as the $[Ca^{2+}]i$ increases. There are several cytosolic Ca-binding proteins such as TnC (Ca^{2+} and Ca^{2+}/Mg^{2+} binding sites), myosin, SERCA, calmodulin, ATP, creatine phosphate, parvalbumin (which is present only in fast-twitch muscle and responsible for its rapid relaxation) and other sarcolemmal sites (Bers, 2002). According to Bers (Bers, 2002), one of the main ways of changing the strength of cardiac contraction is by altering the amplitude or the duration of the Ca^{2+} transients. A correlation between SR calcium content and intracellular Ca^{2+} transients has been reported, with a decreased SR Ca^{2+} release in a low SR calcium content scenario (Bers, 2002). Because of the alleged implication of Ca^{2+} handling in some pathologies, such as heart failure and muscle dystrophy (discussed in the following paragraphs) there has been a growing interest in studying calcium behavior.

4. Role of calcium in heart failure and muscle dystrophy

Heart failure (HF) is a leading cause of death in Western civilization and, although there are different features characterizing this syndrome, some common ones are a prolongation of the QT interval, progressive depression of basal cardiac contractility and loss of inotropic reserve (Piacentino *et al*., 2003). Several attempts have been made to understand the mechanisms underlying HF but the cellular basis is not completely understood. It is generally agreed that much of the contractile deficit is due to an aberrant intracellular calcium handling, which leads to reduced Ca^{2+} transients (Piacentino *et al*., 2003; Lindner *et al*., 1998, Diaz *et al*., 2005, *Bers et al.*, 2003, Neef & Maier, 2013). The most popular explanation for reduced Ca^{2+} transients is a reduced SR Ca^{2+} content (Piacentino *et al*., 2003; Lindner *et al*., 1998, Diaz *et al*., 2005, *Bers et al.*, 2003, Hobai *et al.*, 2001), although the reason behind this reduction is still controversial. Some groups found enhanced NCX expression and activity, which would increase the extrusion of Ca^{2+} towards the extracellular compartment (i.e., Hasenfuss, 1988). A lower expression or activity (i.e., Hasenfuss, 1988; Meyer et al., 1995) of the SERCA pump, in some cases due to a lower phosphorylation of the phospholamban (i.e., Schwinger *et al*., 1999), has also been reported. Finally, an altered activity of the RyR_2 leading to a calcium leak is thought to contribute to a reduced SR Ca^{2+} content.

Duchenne muscle dystrophy (DMD) has also been of interest for those studying calcium pathologies. DMD is a X-linked recessive disease affecting 2 – 3 per 10000 males in the world population (Yoshida *et al.*, 2006) and characterized by a lack of dystrophin (a protein linking the sarcolemma with the cytoskeleton), which causes a series of events that are not completely understood and that lead to muscle weakness due to fiber necrosis and fibrosis (Fraysse *et al*., 2004). Although not unanimous, the hypothesis of an increase of the $[Ca^{2+}]i$ leading to a pathological condition referred to as “calcium overload” is the most accepted one when trying to explain the conditions leading to muscle destruction (Fraysse *et al.*, 2004; Mazala *et al*., 2015; Yoshida *et al*., 2006). This increase in intracellular calcium would lead to the activation of certain proteins such as calpains (Belcastro, 1993), a family of proteases in charge of the degradation of certain intracellular structures such as the RyR (Singh *et al.*, 2004) and the junctophilin-1 (Murphy et al., 2013), a protein that has a role in the proper formation and maintenance of the triad junction (Landstrom et al., 2014). Mazala *et al*. (2015) suggested that the weakness of skeletal muscle in DMD patients is due to E-C

coupling failure as a result of the degradation of these essential structures (Mazala *et al*., 2015).

Although the mechanism underlying a poor intracellular calcium handling in these pathologies is still to be described, measurement of [Ca_T] in the intracellular space has been of particular interest and several attempts have been made in order to establish accurate values for both skeletal and cardiac muscle.

5. Calcium measurements in the heart

As mentioned before, due to the importance of calcium in muscle contraction and intracellular signaling pathways (among others) and its implication in pathologies such as the ones described in the preceding section, the study of calcium behavior has been of great interest. Some of the characteristics researchers look at are calcium transients, intracellular calcium buffers and intracellular and extracellular free calcium and total calcium concentrations in skeletal and cardiac muscle tissue (denoted [Ca_T]). Kirbi *et al*. (1975, 1981) and Gissel & Claussen (1999) give some examples of [Ca_T] measurements in frog and rat skeletal muscle. Frog EDL calcium content was measured by equilibrating the sample with Ca^{45} (Kirbi *et al.,* 1975). In the case of rat skeletal muscle, [Ca_T] has also been estimated using atomic absorbance spectroscopy (AAS), a technique where the sample is burned, and the calcium measured by its atomic absorbance spectrum (Kirbi *et al*., 1981; Gissel & Claussen, 1999). There are some issues related to the use of these techniques. The main issue regarding the technique involving Ca^{45} is the loss of calcium during the sample equilibration with Ca^{45} which would lead to an underestimation of the actual calcium content. In the case of the AAS, the process is long and the estimation of [Ca_T] can have associated an important error due to the calibration that the method requires. However, in general, there is an agreement regarding [Ca_T] in mammal skeletal muscle.

Several attempts have also been made to measure [Ca_T] in cardiac tissue. In 1995, Bassani and Bers performed total calcium measurements on chemically and mechanically isolated rat and rabbit cardiomyocytes (Bassani & Bers, 1995). In these experiments, total SR calcium content was estimated from the [Ca]i transients evoked by caffeine. The authors reported values of 114 µmol / L cytosol and 106 µmol / L cytosol for rat and rabbit, respectively. However, as explained in detail later in this document, our results (presented in this study) indicate that [Ca_T] in the heart is, actually, about 27 times higher. These results

were obtained by using a new method recently developed in our lab (Lamboley *et al*., 2015). Interestingly, calcium content of isolated fibers from frog skeletal muscle, agrees with $[Ca_T]$ measured from whole muscle. It is also noted that $[Ca_T]$ measured by Lamboley *et al.*, (2015) also agrees with measurements with other methods, though there was a very large discrepancy between how much Ca^{2+} comes from the intracellular vs. the extracellular space.

6. The BAPTA method

This new method uses the difference in the UV absorbance spectra of the Ca-bound and Ca-free forms of the Ca-chelator BAPTA. A mouse muscle sample is manually homogenized with a solution referred to as measurement solution (MS), containing the calcium-chelator BAPTA and SDS, a detergent used to permeabilize biological membranes. The resulting product is centrifuged, and the supernatant recovered. At this point, the calcium present in the solution (mostly, coming from the muscle sample) is bound to the BAPTA which, when measured in a spectrophotometer, will give a specific absorbance spectrum that the authors call A_M (the subscript referring to *muscle*). After the first measurement, another calcium-chelator, the EGTA, is added to the sample and the absorbance is measured. Under the conditions presented by the authors, the EGTA has a higher affinity for the calcium than the BAPTA and it is added in a much higher concentration. Because of this, EGTA displaces essentially all of the calcium from BAPTA causing a change in BAPTA absorbance. This absorbance is called A_0, the subscript referring to *0 Ca* bound to BAPTA. Finally, a high concentration of calcium is added in another aliquot of the original solution, which causes all the BAPTA to bound calcium and the absorbance is measured (A_∞, the subscript referring to infinite calcium). A program was developed to process the previously mentioned sets of absorbance data (A_M, A_0, A_∞), as well as a set of equations using the data obtained together with other parameters such as the muscle weight, the volume of the original solutions and the volume of the aliquots in order to calculate $[Ca_T]_{WM}$. These equations were based on several assumptions explained in Lamboley *et al.* (2015) and they are based on the Lambert-Beers's Law.

Equation A_M is given by

$$A_M = A_{INTR} + \left\{ \begin{matrix} \varepsilon_{CaB}\left([CaB]_M + [CaB]_{background}\right) + \\ \varepsilon_B\left([B_T] - [CaB]_M - [CaB]_{background}\right) \end{matrix} \right\} \cdot l \quad (1)$$

where A_{INTR} is the intrinsic absorbance, [Ca*B*]$_M$ and [Ca*B*]$_{background}$ are the concentrations of the Ca-bound form of BAPTA, when the calcium comes from the muscle (*M*) and from places other than the muscle (*background*), respectively, ε_{CaB} and ε_B are the extinction coefficients of the Ca-bound and Ca-free forms of BAPTA, respectively and *l* is the pathlength. Likewise, A_0 and A_∞ are given by

$$A_0 = A_{INTR} + \varepsilon_B[B_T] \cdot l \quad (2)$$

$$A_\infty = A_{INTR} + \varepsilon_{CaB}[B_T] \cdot l \quad (3)$$

where $[B_T]$ is the total BAPTA concentration and is determined by the difference between A_∞ and A_0 substituted and the difference between equations 2b and 2a (see Lamboley et al., 2015 for further explanation). From the two previous equations and assuming A_{INTR} to be the same in both, one can obtain the following equation

$$\frac{A_M - A_0}{\Delta\varepsilon \cdot l} = [CaB]_M + [CaB]_{background} \quad (4)$$

where $\Delta\mathcal{E} \equiv \mathcal{E}_{CaB} - \mathcal{E}_B$. [CaB]$_{background}$ is determined by performing the same kind of measurement only with no muscle sample present (see Lamboley *et al.*, 2015 for more information). Finally, calcium content of the muscle ($[Ca_T]_{WM}$, the subscript *WM* standing for *whole muscle*), in units of millimoles of calcium per kilogram of muscle, can be estimated as follows:

$$[Ca_T]_{WM} = \frac{V_{solution}}{W_{muscle}}[CaB]_M \quad (5)$$

where $V_{solution}$ is the volume of MS added to the sample combined with the weight of the muscle sample and W_{muscle} is the weight of the muscle.

Equations 1, 2, 3, 4 and 5 correspond to equations 1, 2, 3, 5 and 17 in Lamboley *et al.* (2015), respectively.

One of the advantages of this new method is the capability of obtaining precise $[Ca_T]_{WM}$ estimations. However, this method is also time consuming, since the samples to measure need to be grinded manually (which takes around 7 minutes per samples) and the absorbance is measured with a spectrophotometer, which allows the measurement of one sample at a time. Because of this, we've more recently adapted the BAPTA method to the use of a plate reader, which allows the analysis of multiple samples at a time. We've also introduced a commercially available grinder to replace the manual grinder. A major part of my work during my M.Sc. training involved working out several issues associated with these modifications of the protocol, some of which are presented later.

7. Early results from our lab

By using this new method, Lamboley *et al*. (2015) studied the relationship among the calcium content of a given muscle ($[Ca_T]_{WM}$) and the ratio between the weight of the mouse and the weight of that muscle. Interestingly, they noticed that $[Ca_T]_{WM}$ increases as the ratio mouse weight/ muscle weight increases, a condition found in the mouse fast-twitch muscle EDL and slow-twitch muscle soleus (Sol) (Lamboley *et al.*, 2015). We, then, hypothesized that the muscle is "sensing" that a given level of force is required, and it is capable of upregulating its intracellular calcium load in order to give an appropriate response. This would, in this case, help small muscles (relative to the mouse weight) compensate for the force demands. The potential importance of this observation is the possible existence of one (or several) physiological mechanism(s) by which muscle cells upregulate their intracellular calcium content in other to respond to the functional demands of the tissue. This hypothetical mechanism might be important to improve our understanding of some Ca-related pathologies such as muscle dystrophy, where the muscular tissue is replaced by

connective tissue, which causes a muscle deficit. In this scenario, the muscle would try to compensate for the deficit by increasing intracellular calcium, which would lead to an enhanced apoptotic activity. This would worsen the original condition, which would cause more calcium to come into the cell, producing a vicious cycle situation. Understanding such a mechanism in skeletal muscle and its potential to lead to Ca-overloading is likely to have some relevance to other pathologies related to Ca-overload such as heart failure, Alzheimer's disease and Huntington's disease.

Rather than simple, this hypothetical mechanism could be a process involving several structures operating at many different levels. Because of this, our first aim was to find a set of reproducible conditions that would cause sort term changes in calcium content. Our main lead came from the results obtained from a set of experiments performed in our lab. They indicate a possible role for stress and/or exercise in increasing total calcium in muscle tissue (McDonell & Pape, 2015). When measuring $[Ca_T]_{WM}$ in skeletal and cardiac tissue, a difference was found between a group of control mice and a group of mice that were reported to look very agitated and that were constantly moving around and climbing inside of their cage. Table 1 shows measured $[Ca_T]_{WM}$ of both control and "agitated" groups. The authors reported a statistically significant difference among $[Ca_T]_{WM}$ between both groups in the case of the EDL and the Sol.

The goal of this study is to find a set of reproductible conditions involving adrenergic stimulation and exercise and affecting $[Ca_T]$ in the skeletal and cardiac muscle. For this aim, we also propose an adaptation of the BAPTA method to the use of a plate reader to perform faster and more accurate measurements.

	$[Ca_T]_{WM}$ (mmol / kg wet muscle)		RATIO
	Rested mice	**Active mice**	
EDL			
Average	2.25	4.05	1.80
SEM	0.293	0.452	
N	8	8	
SOL			
Average	2.32	2.42	1.04
SEM	0.766	0.232	
N	7	7	
HEART			
Average	1.42	2.67	1.88
SEM	0.0313	0.251	
N	10	10	

Table 1. Preliminary results from Dr. Pape's laboratory. $[Ca_T]_{WM}$ of muscles e*xtensor digitorum longus*, (EDL), soleus (SOL) and the heart was measured using the BAPTA method (Lamboley *et al.*, 2015). Differences between a group of rested mice and a group of mice that were climbing inside of their cage and moving around (referred to as "active" mice) are shown. The ratio establishes the comparison between the two groups. Biophysical Journal Vol. 110, Issue 3. 60th Annual Meeting of the Biophysical Society, Los Angeles, California, United States (99a). Data obtained by Abby McDonell.

MATERIALS AND METHODS

1. Animal ethics

All the procedures were conducted under a protocol approved by the CFPA-FMSS (Comité facultaire de protection des animaux de la Faculté de médicine et des sciences de la santé) of Université de Sherbrooke.

2. Animal model

A mouse model (C57BL/6 females, aged 64 – 72 days) was used in all the experiments preformed.

3. Animal handling

For all the experiments explained in this document, mice were anesthetized by isoflurane and, immediately after, euthanized by cervical dislocation.

4. Composition of the solutions

The composition of the main solution, referred to as measurement solution (MS) is as follows: 0.2 mM BAPTA, 2 mM HEPES, 2 mM $MgCl_2$, 120 mM NaCl. The solution was titrated with NaOH to pH 8. Before being dried and weighted, muscles were generally placed briefly (~2 - 3 sec) in mammalian Ringer's solution whose composition was as follows: 1.8 mM $CaCl_2$, 5 mM KCl, 146 mM NaCl, 1mM $MgCl_2$ and 10 mM HEPES titrated with NaOH to pH 7.4. A calcium-free sodium-free modified mammalian Ringer's solution (5 mM KCl, 10 mM HEPES, 1 mM $MgCl_2$, 146 CholineCl, 1 mM EGTA) was used to wash out the extracellular calcium in some cases (as described later). All modified physiological solutions were titrated with NaOH to pH 7.4 and the osmolarity was adjusted to 295 mosm.

Two solutions consisting of 0.3 and 0.6 mM Ca in MS were also prepared as a calibration system of the BAPTA method.

5. Establishment of conditions to determine the effect of adrenergic stimulation or exercise on calcium content and muscle tissue preparation

36 mice were assigned to one of the following groups: control (CON), epinephrine injection (EPI), saline injection (SAL), exercise (Ex), epinephrine injection and exercise combined (EPI+Ex) and saline injection and exercise combined (SAL+Ex). N = 6 in each of the groups.

The effect of the adrenergic stimulation was studied by the application of an epinephrine injection, as indicated by the name of the group of mice that underwent this treatment. Mice were injected intraperitonially with 0.017 mL/gram of mouse weight of a solution containing epinephrine at 12 mg/mL in 0.9% NaCl. This would give a final epinephrine concentration in the mice of 0.204 mg/mL. Saline injections consisted on 0.017 mL/g of 0.9% NaCl.

The effect of exercise on calcium content was tested by using a rodent treadmill (LE 8700 Series, Panlab Harvard apparatus). For determining the speed and duration of the exercise as well as for acclimating the mice to the use of the treadmill, two training sessions were performed about 1 week before the day of the test. The goal of Session 1 was to determine the maximal speed that each mouse can achieve. For that aim, the mouse was placed on the treadmill, and the speed was increased gradually until the mouse was not capable of keeping up with the speed. Session 2 took place 24h after Session 1. The goal was to determine the duration of the exercise and to allow further acclimation to the treadmill. For that aim, the speed was increased gradually to 80% of the maximal speed achieved during Session 1. The mice were then left to run for a maximum of 10 min. The time was noted when the mouse could no longer keep up with the exercise or at 10 min. The test, 7 days after Session 2, was done at 80% of the maximal speed achieved by each mouse, determined in Session 1, for a period of time corresponding to the time measured in Session 2, or longer.

It is noted that group CON did not undergo these two training sessions since we assume that there would be no difference between a control group that underwent this acclimation period and the one we used in our experiments, which was not trained. This seems like a reasonable assumption, since it seems that any hypothetical effect of physical activity on $[Ca_T]_{WM}$ should wear off in a matter of hours.

Group CON was brought to the laboratory from the animal facility and left for at least one hour to acclimate. After the acclimation, one mouse was euthanized, followed by the euthanasia of a second mouse before proceeding to the extraction of muscle for both mice.

The reason behind this is avoiding muscle drying, which might happen if all the mice were euthanized at the same time. EPI and SAL groups went through the same steps, with the addition of an epinephrine or saline injection 30 min prior to euthanasia. Group Ex followed the two training sessions and was euthanized immediately after the test. Groups EPI+Ex and SAL+Ex were injected with epinephrine and saline, respectively, 20 min prior to the 10-min exercise protocol.

Muscles *extensor digitorum longus* (EDL), soleus (Sol), biceps (BCP) and *brachioradialis* (BR), ranging from 4 to 21 mg, were collected from tendon to tendon within a range of 30 to 90 min after the euthanasia. The whole heart was also taken and weighted and three samples between 6 and 17 mg corresponding to the apex, the left ventricle and the atriums were collected. The skeletal samples were taken with as little tendon as possible without affecting the muscle. Both skeletal and cardiac samples, unless otherwise is indicated, were briefly placed in the mammalian Ringer's solution for 2 – 3 seconds prior to being blotted dry in 1.5 mL polypropylene microcentrifuge tubes and weighted. The tubes contained 8 Teflon balls (1/8" PTFE Solid Plastic Balls, US Plastic), used for the homogenization of the tissue in MS. In all cases, the samples were frozen in the previously mentioned tubes for later processing. The homogenization was performed with 0.2 mL of MS added to the tube in an automatic grinder (BeadBug Microtube Homogenizer, Benchmark Scientific, US). 1.5 mL of MS were added after the homogenization to give a final volume of 1.7 mL, as well as SDS to give a ~0.5% concentration in the tube. The SDS is necessary to dissolve surface and T-system membranes as well as for protein denaturation. The final volume in the tube was calculated by weight, by subtracting the previously measured weight of the tube containing the grinding balls, assuming a density of 1 g/mL. Samples were centrifuged at 13300 rpm for 30 min at 6ºC to remove insoluble muscle components that would give a high intrinsic absorbance or light scattering.

6. Removal of extracellular calcium in heart samples

A sample of every heart used for the determination of the effects of adrenergic stimulation and exercise was left for 30 minutes in a Ca-free, Na-free modified mammalian Ringer's solution and later dried, bottled and processed as described above.

7. Absorbance measurements

For the absorbance measures, a 96-well Glass Bottom MicroWell plastic plate (model MGB096-1-1-LG-L; MatriCal, Inc., Spokane, WA, USA) conforming the standards to be used in a Tecan Infinite® M1000 plate reader was used. In order to perform the measurements detailed below, different compounds need to be added to different aliquots of the same sample, so two wells of the plate were required for each muscle sample. The volume of each aliquot added to the well was 300 µL at the beginning of the first measurement. The previously mentioned Tecan Infinite® M1000 device was used to perform the measurements. The absorbance measurements are determined from changes of intensity of the light that passes through the glass bottom of the plates and the solution added to the well.

Four absorbance measurements are done on each set of samples, namely A_M, A_0, A_S and A_∞. Two wells are used per sample to perform these measurements. A_M and A_0 are determined in the first well. In the second well, A_M is also measured, followed by A_S and A_∞. Every measurement is repeated twice and is preceded by 30 seconds of shaking, followed by 2 min of pause. These parameters can be set in the plate reader. As explained earlier in this document, A_M represents the absorbance of the solution obtained from the tubes after the centrifugation with no further processing. *A0* is determined by the addition of EGTA to one of the aliquots, in order to displace all the calcium from the BAPTA, as EGTA is added in a much larger concentration than BAPTA. The EGTA concentration in the well is 2 mM, which should be enough for the EGTA to complex > 99.5% of the total calcium present (see the Appendix section in Lamboley *et al.*, 2015). A_S is obtained by including a known amount of calcium standard to the second aliquot, in this case, 0.03 mM Ca. This measurement is used as calibration of the method. $A\infty$ is determined by adding excess calcium (the final concentration in the well is 2 mM Ca) to the A_S so that all the BAPTA present is in the Ca-BAPTA form. A pair of wells is reserved to be filled with water, which will be used as blank. One of the rows of the plates (6 pairs of wells) are use for a second calibration system. They are filled with either 0.3 or 0.6 mM Ca MS and measured with the samples, being treated as a regular sample.

Some steps need to be followed before analyzing the samples in order to improve the accuracy of the measurements performed. Before the samples are measured, the calcium that is not coming from the samples (background Ca) needs to be eliminated as much as possible. We follow a cleaning protocol where the plate is rinsed 6 times with low resistance

water, filled with MS and left for 5 min (so the calcium present can bind the BAPTA present in the MS) and rinsed again 3 times with low resistance water. This protocol is applied before and after every measurement perform on the plate. The fraction of calcium that is not coming from the samples ($Ca_{background}$) is determined by filling the plate that will be later used to measure the absorbance of the samples with MS and performing the measurements explained in the paragraph above (A_M, A_0, A_s, A_∞), only with no muscle present. This set of measurements is called *before values* and, as explained in Lamboley *et at*., (2015), the single measurements are referred to as S_m, S_0, S_s and S_∞. After the $Ca_{background}$ is measured, the plate is used to measure the samples. $Ca_{background}$ is determined once again (*after values*) in a last step.

8. $[Ca_T]_{WM}$ determination

Calcium content of the samples was estimated by following the formulae described briefly above and in detail in Lamboley *et al.* (2015). The main ones used are equations 1, 2, 3 and 4 in this document (see introduction), corresponding to equations 1, 2, 5 and 17 in Lamboley *et al.* (2015).

As in the original paper, $Ca_{background}$ values are determined by performing the same kind of measurement only with no muscle sample present. However, as explained in the first subsection of the results in this document, since the method has been adapted to the use of the plate reader, the background is now specific for each set of wells of the plate. See the Results section for more details.

9. Data analysis

The results of each of the sample were studied individually and discarded in the case where a human error was spotted (i.e. one of the elements was not added during the absorbance measurements).

A one-way ANOVA test was run to compare the results obtained from the CON, EPI and SAL groups. Since this test shows if there is a statistically significant difference among treatments, but it does not indicate which pairs of treatments are different from each other, a post-hoc Tukey HSD Test was used to complete the analysis.

A one-way ANOVA test followed by a post-hoc Tukey HSD Test were also run to compare the results obtained from the EPI, SAL, EPI+Ex and SAL+Ex groups.

Finally, CON and Ex results were compared with a one-way ANOVA test.

For both tests, two significance levels are applied: $p<0.05$, which suggests a statistically significant difference and $p<0.01$, which suggests a strong statistically significant difference.

RESULTS

1. Adaptation of the BAPTA method to the use of a plate reader for absorbance measurements

Before the final protocol (described in the Materials and Methods section in this document) concerning the treatment and analysis of muscle samples in order to measure $[Ca_T]_{WM}$ was established, several issues had to be resolved in order to obtain accurate values. The following paragraphs summarize chronologically the steps followed and the difficulties faced in the process of the protocol development.

1.1 Handling $Ca_{background}$ coming from the plates and other materials

It is mentioned in Lamboley's publication (2015) that the calcium present in the solution has diverse origins. Although most of it comes from the muscle, calcium is also present in the materials used to perform the measurements and it is imperative to measure it. Determination of $Ca_{background}$ has been one of the hardest tasks to accomplish.

The most likely sources of calcium contamination are the MS itself (calcium can leach from the materials used to prepare it) and the plates used for measuring the absorbances. Since getting rid of the calcium is not likely an option, the solution given to handling it was to measure it. For this aim, several methods were tested until the final protocol was described. Our first approach was to use a pair of wells filled with MS as background. These wells are treated as regular samples and the absorbance measurements are called S_m, S_0, S_∞ to be consistent with the nomenclature used by the original authors. For convenience, binding is often expressed in terms of the fraction of BAPTA bound with calcium, which is denoted *"f"* by the authors of Lamboley *et al.*, 2015. *f* is defined by the following expression:

$$f = \frac{A_M - A_0}{A_\infty - A_0} \tag{6}$$

This equation was determined from equations 5, 6 and 9 in Lamboley *et al*., 2015 and corresponds to equation 13 in the same document.

f can be defined as sum of two parts: calcium coming from the muscle and calcium coming from the background, so it can also be expressed as follows:

$$f = f_M + f_{background} \tag{7}$$

where

$$f_M \equiv \frac{[CaB]_M}{[B_T]} \tag{8}$$

and

$$f_{background} \equiv \frac{[CaB]_{background}}{[B_T]} \tag{9}$$

Another useful way of expressing $f_{background}$ is:

$$f_{background} = \frac{S_M - S_0}{S_\infty - S_0} \tag{10}$$

where S_m, S_0 and S_∞, as previously mentioned, correspond to the same measurements performed with the muscle samples, only with no samples present. Equations 7, 8, 9 and 10 of this document, correspond to equations 10, 11, 12 and 14 in Lamboley *et al.,* 2015.

Lamboley *et al.* (2015) reported similar calcium content for left and right EDL and soleus muscles belonging to the same mouse. When our preliminary results were obtained, the same analysis was done. However, our values looked very scattered (Fig. 4). Another type of data analysis came to confirm a problem with the background. For our experiments, 3 heart samples were collected, and each of them was split in two. The 6 samples were measured, $[Ca_T]_{WM}$ was calculated, and the results compared. Similar $[Ca_T]_{WM}$ values are expected from samples coming from the same regions of the heart. Fig. 5, however, indicates otherwise. Since the scatter of data indicated a problem with the method, several

changes in the protocol were tried to fix this problem. In the first attempt, we used an entire row of wells, only to find that $Ca_{background}$ is very variable among wells and that it also varies within the same well, with every use of the plate (Fig. 6). Since this variability cannot be controlled, another solution to use every pair of wells as their own blank. For that aim, $Ca_{background}$ is determined for each well before and after the measurement of the samples and the $[Ca_T]_{WM}$ of each sample is corrected for the average of those two measurements. This approach worked since $f_{background}$ values for a given well did not change much, as evidenced by matches between the before and after background measurements (not shown).

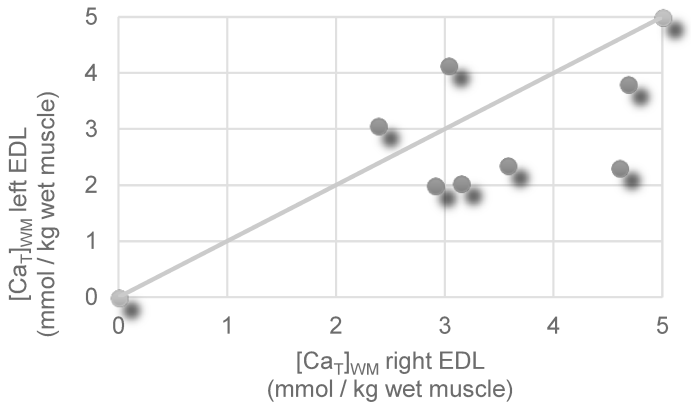

Figure 4. **C**omparison between $[Ca_T]_{WM}$ values obtained from left and right mouse EDL. The line represents a unity line. The closer the dots are to the line, the more similar the left and right EDLs are in terms of $[Ca_T]_{WM}$ values.

Figure 5. Comparison of $[Ca_T]_{WM}$ values from samples coming from the same region of the heart. Two samples from a given region of the heart are taken and their calcium content compared. The scatter from the unity line indicates that paired samples from the same heart region did not usually give the same results, as expected.

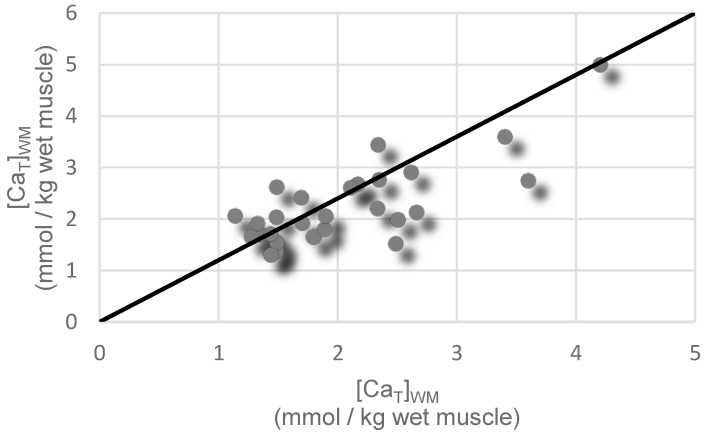

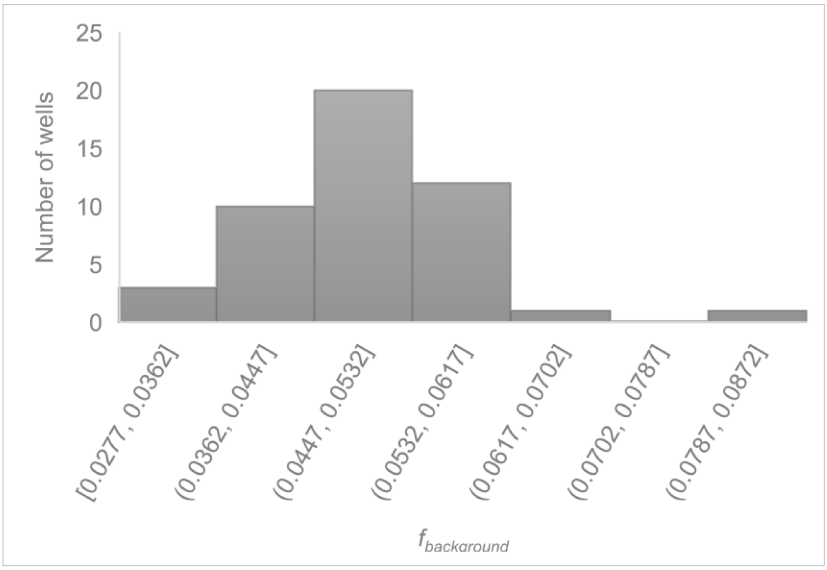

Figure 6. $Ca_{background}$ measurements. Calcium background from 47 wells is measured and the results, expressed in terms of fraction, are grouped in seven groups limited by specific ranges, indicated in the horizontal axis. The vertical axis indicates the number of wells fitting in each group.

1.2 Replacing manual grinding with automatic grinding

As mentioned before, a secondary adaptation concerning the grinding of the samples has been made to the original protocol. The samples, so far grinded manually one at a time, are now grinded automatically in groups of three (Fig. 7).

When skeletal and heart samples are collected, they are bottled in centrifuge tubes previously prepared containing 8 stainless steel balls (2.8 mm diameter; OPS diagnostics grinding balls) each. 200 µL of MS are later added to each sample and three tubes at a time are placed in the automatic grinder (1/8" PTFE Solid Plastic Balls, US Plastic). For the aim of our study, the grinder is set to 30 seconds at maximal speed.

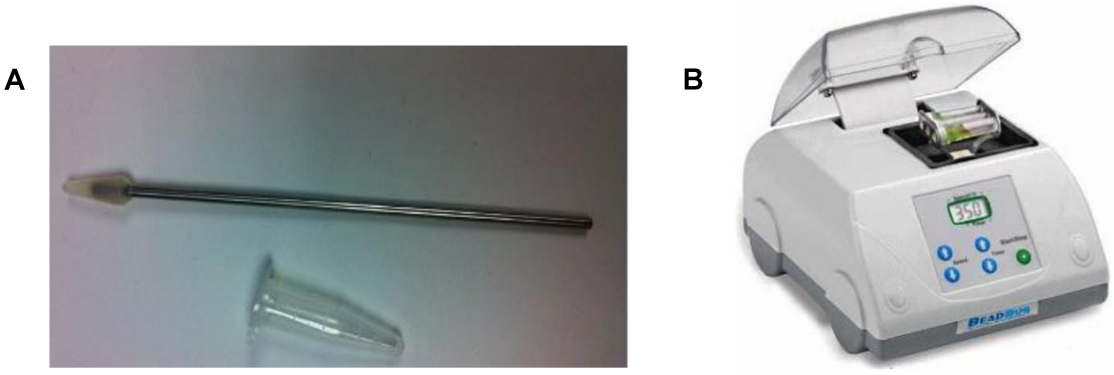

Figure 7. Manual and mechanical grinders. Fig 7A represents a manual grinder, used in the original protocol (Lamboley *et al.*, 2015). Fig 7B is BeadBug Microtube Homogenizer).

1.2.1 Stainless Steel Balls

Another important source of $Ca_{background}$ is the grinding balls. One of the properties of the stainless-steel balls (Fig. 8A) that made them appealing for this study, is that calcium was not expected to leach from them. The protocol followed to obtain our preliminary results included the use of this type of balls. However, suspicion arouse that calcium might have been leaching from them and contaminating our samples, although some other components (such as the aluminum, which also binds to BAPTA) present in this type of balls might also be the cause of contamination. The first attempt to address this problem was to redesign the washing protocol used on the balls. For this aim, different groups of stainless-steel balls were rinsed several times in deionized water and left in different compounds. The fact of the stainless-steel balls being reused for every experiment (these balls are referred to as old stainless-steel balls) has also been questioned. Fig. 9 shows the calcium concentration measured from 1) new stainless-steel balls rinsed with deionized water, 2) old (already used) stainless-steel balls rinsed with deionized water, 3) old stainless-steel balls rinsed with deionized water and left in clean deionized water, 4) old stainless-steel balls rinsed with deionized water and left in MS and 5) old stainless-steel balls rinsed with deionized water, "grinded" with SDS during 1 min and later rinsed with a 0.9% NaCl solution. Unexpectedly, old balls showed lower calcium concentration than new balls, most likely due to the use of MS during the sample processing, which includes the Ca-chelator BAPTA. Among the old stainless-steel balls, those "grinded" with SDS and later rinsed with NaCl showed the lowest $Ca_{background}$ levels. Although the washing protocol was initially changed to include the use of SDS + NaCl, the SDS caused the stainless-steel balls to get rusted. Despite successfully reducing $Ca_{background}$ with stainless-steel balls, the appearance of rust (Fig. 9A) led us to abandon the use of stainless-steel balls and try another type of balls. Other types of balls offered by the manufacture, including ceramic balls, also caused problems. We, therefore, decided to try Teflon balls, obtained from another source.

1.2.2 Teflon Balls

Since no washing protocol was suitable enough, another type of balls, Teflon balls (see Fig. 8B), was tested. Teflon is an appreciated material in our laboratory since calcium does not significantly leach from it. Two questions arouse concerning the usefulness of the Teflon balls: whether the amount of calcium leaching from them is negligible and whether they are

suitable for muscle grinding. Teflon balls proved to be suitable for muscle grinding. However, whereas with the stainless-steel balls we were spending 30 seconds per sample, with the Teflon balls it takes between 3 and 8 minutes. It is noted that samples can still be grinded in groups of three so, overall, the process is still faster than it was with the manual grinder. Calcium coming from new Teflon balls was measured and compared to that coming from new stainless-steel balls. Fig. 10 shows the results obtained. As expected, calcium levels of the Teflon balls were fairly low and, more importantly, constant for all the groups of balls used. When compared to the stainless-steel balls, Teflon balls represent an important improvement.

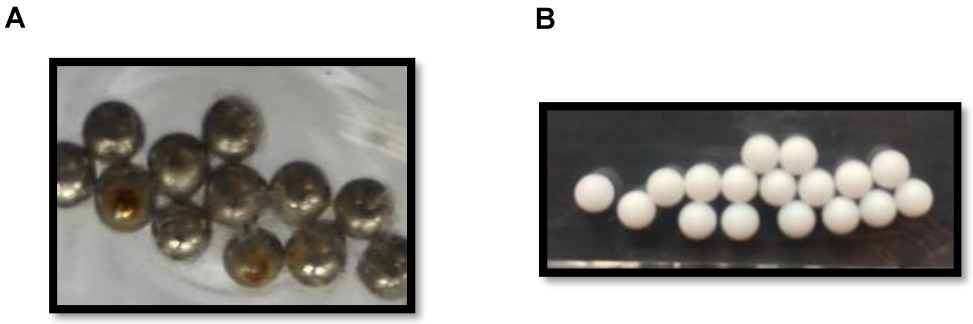

Figure 8. Rusted stainless steel balls and Teflon balls. Fig. 8A represents the stainless-steel balls as they were after being cleaned with SDS and rinsed with a 0.9% NaCl solution. Notice the rust. Fig. 8B is a picture of the Teflon balls used as an alternative to the stainless-steel balls.

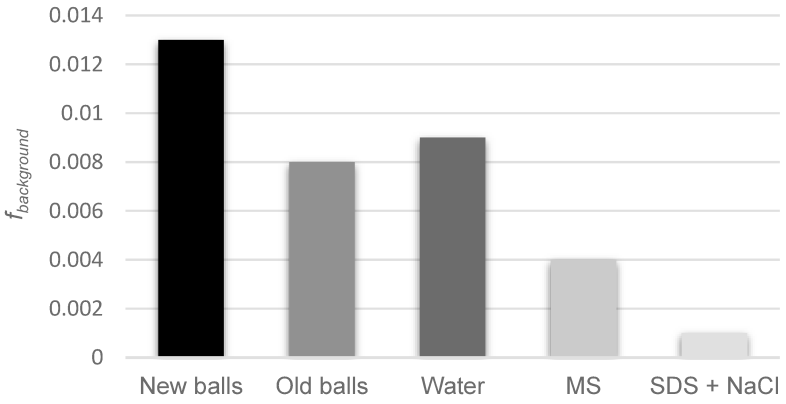

Figure 9. Comparison between $f_{background}$ values of different sets of balls. Different groups of balls are cleaned differently, and the calcium background measured and expressed in terms of fraction. The different groups are: 1) new balls, 2) old balls that had been previously rinsed with low resistance water, 3) old balls rinsed with low resistance water prior to the measurement and 4) old balls rinsed with measurement solution and 5) old balls left in SDS and later rinsed with a 0.9% NaCl solution.

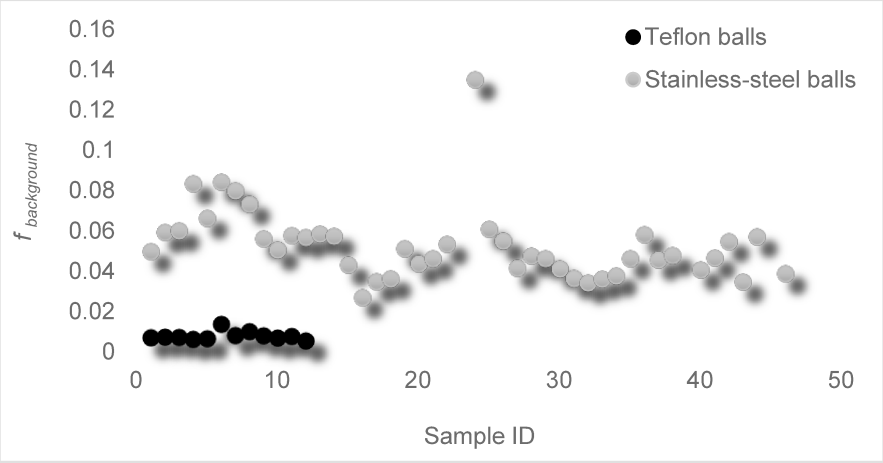

Figure 10. $f_{background}$ results from a series of measurements of stainless-steel balls and Teflon balls. Stainless-steel balls and Teflon balls were divided in 46 and 12 groups of 8 balls (respectively) and the calcium concentration was calculated using the BAPTA method. Notice how Teflon balls give much lower values, making them more suitable for our experiments.

2 $[Ca_T]_{WM}$ measurements

As explained previously, calculating $[Ca_T]_{WM}$ requires three measurements per sample, the first one corresponding to $Ca_{background}$ (with no muscle sample present), the second one to $[Ca_T]_{WM}$ (with a muscle sample present) and the third one also corresponding to $Ca_{background}$. As a reminder, the first and third measurements are averaged to give a single $f_{background}$ value. Fig. 11 shows the typical spectra obtained from the $[Ca_T]_{WM}$ measurement of one skeletal muscle sample and its corresponding $f_{background}$ (in this case, only one $f_{background}$ measurement is shown). Fig. 11A and B represent the results obtained from a mouse right EDL $[Ca_T]_{WM}$ measurement and C and D correspond to a $Ca_{background}$ measurement, obtained in the same way as A and B only with no muscle present. The four absorbance measurements (A_M, A_0, A_S, A_∞ or S_M, S_0, S_S, S_∞) are plotted in A and C. A_S and S_S represent both a $[Ca^{2+}]$ of 0.03 mM. B and D show the following differences: $A_0 - A_\infty$, $A_M - A_S$ and $A_0 - A_M$. Absorbance with the lower level of calcium present minus that with the higher level, to give positive values. As stated in Lamboley *et al.*, (2015), the reason behind this inconvenience is that the Ca-free form of BAPTA has a higher absorbance than the Ca-bound form. A_M - A_0 has the most important information, since it is proportional to the total Ca^{2+} bound to BAPTA ($[CaB] = [CaB]_M + [CaB]_{background}$) (Eq. 4). As noted in the Methods, it was more convenient to express this concentration as the fraction of BAPTA that has calcium bound to it (Eq. 6). Fig. 11B shows the least-squares best fit of the $A_0 - A_M$ difference spectra to the corresponding

$A_0 - A_\infty$ data (represented by the solid blue line). The green curve shows the least-squares best fit of the $A_M - A_S$ difference to the $A_0 - A_\infty$ difference. The same applies to Fig. 11D, where the nomenclature changes to S_M, S_0, S_S and S_∞, since no muscle sample is present. According to Eq. 6, the fraction of BAPTA bound to Ca^{2+} (f) is given by $(A_M - A_0) / (A_\infty - A_0)$, which is the best fit scaling factor giving the blue curve in Fig. 11B. Correspondingly, the best-fit scaling factor of $(S_0 - S_M) / (S_0 - S_\infty)$ (or $(S_M - S_0) / (S_\infty - S_0)$) gives $f_{background}$ (Eq. 10). According to Eq.7, the difference between f and $f_{background}$ gives f_M, the fraction of BAPTA with Ca^{2+} coming from the muscle sample. f_M is then used to calculate $[CaB]_M$ ($[CaB]_M = f_M \times B_T$) as explained in Lamboley *et al.*, 2015).

Fig. 12 represents the exact same analysis than Fig. 11, only performed in cardiac muscle. Fig. 12A and B represent the results obtained from a mouse left ventricle $[Ca_T]_{WM}$ measurement and C and D correspond to a $Ca_{background}$ measurement, obtained in the same way as A and B only with no muscle present. Absorbance spectra are similar in both skeletal and cardiac tissue. However, intrinsic absorbance is higher in the case of the heart, as shown in the top left panel (Fig. 12A). Experiments performed with muscle sample but no BAPTA present, indicate that the intrinsic absorbance it is not altered by the addition of EGTA (needed for obtaining A_0), calcium standard (needed for obtaining A_S) or excess calcium (added for the A_∞ measurement) (Fig. 2 and associated text in Lamboley *et al.*, 2015). This justifies the assumption that the intrinsic absorbance cancels out in the different spectra (i. e., Eq. 4).

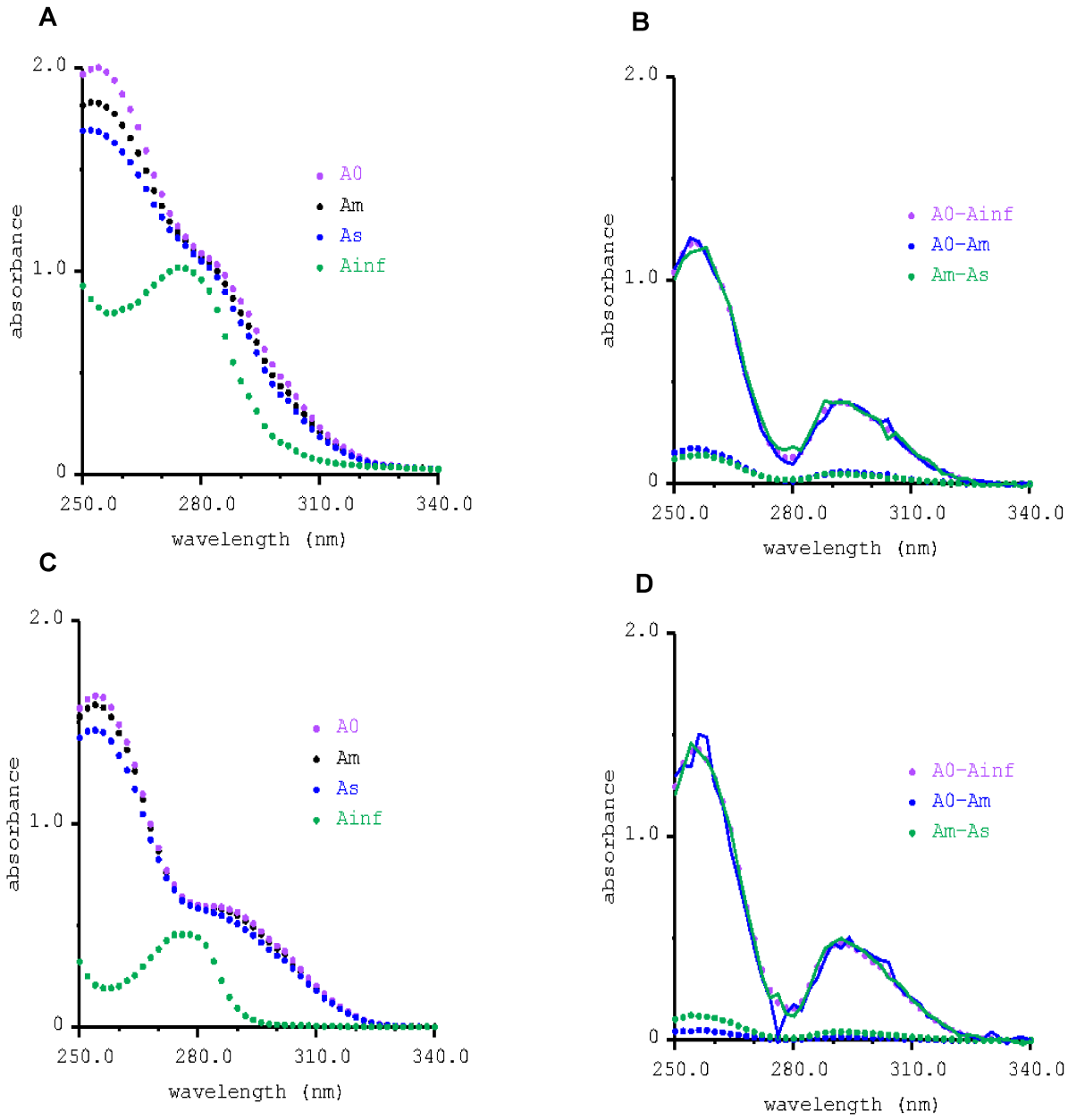

Figure 11. Example of a plot obtained from a $[Ca_T]_{WM}$ analysis in skeletal muscle. The two top plots (Fig. 11A and 11B) were obtained from a mouse right EDL and the two bottom plots (Fig. 11C and 11D) are an example of a calcium background measurement. Fig. 11A corresponds to A_M, A_0, As and A_∞ determination obtained from a mouse EDL. S_M, S_0, S_S and S_∞ in Fig. 11C were obtained by following the same protocol used in Fig. 11A only with no muscle sample present. Both A_S and S_S correspond to a $[Ca^{2+}]$ = 0.03 mM. Fig. 11B shows $A_0 - A_\infty$ (pink circles), $A_0 - A_M$ (blue circles) and $A_M - A_S$ (green circles). The $A_0 - A_M$ difference has been least-square best fitted to the corresponding $A_0 - A_\infty$ data for the full range of spectra (solid blue line) and the $A_0 - A_\infty$ has been least square fitted to the corresponding $A_M - A_S$ data (solid green line), also for the full range of wavelengths used. The same applies to Fig. 11D, where no muscle sample is present. The fraction of BAPTA bound to Ca^{2+} (f) is given by the best-fit scaling factor relating $(A_0 - A_M) / (A_0 - A_\infty)$, which equals $(A_M - A_0) / (A_\infty - A_0)$ (Eq. 6). Correspondingly, the best-fit scaling factor of $(S_0 - S_M) / (S_0 - S_\infty)$ (or $(S_M - S_0) / (S_\infty - S_0)$) gives $f_{background}$ (Eq. 10).

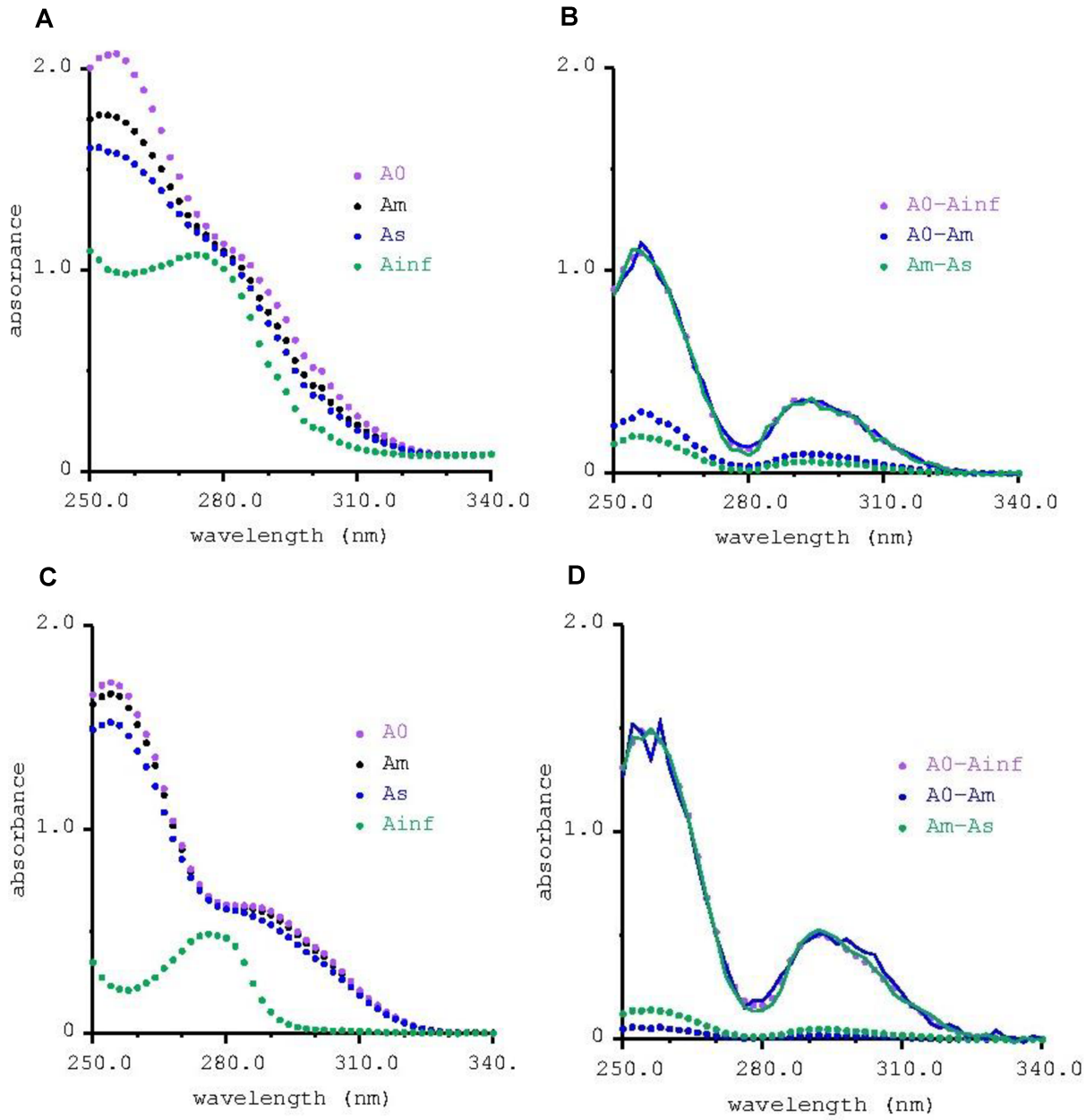

Figure 12. Example of a plot obtained from a $[Ca_T]_{WM}$ analysis in heart muscle. The two top plots (Fig. 12A and 12B) were obtained from a mouse left ventricle and the two bottom plots (Fig. 12C and 12D) are an example of a calcium background measurement. Fig. 12A corresponds to A_M, A_0, A_S and A_∞ determination obtained from a mouse left ventricle. S_M, S_0, S_S and S_∞ in Fig. 12C were obtained by following the same protocol used in Fig. 12A only with no muscle sample present. Both A_S and S_S correspond to a $[Ca^{2+}]$ = 0.03 mM. Fig. 13B shows $A_0 - A_\infty$ (pink circles), $A_0 - A_M$ (blue circles) and $A_M - A_S$ (green circles). The $A_0 - A_M$ difference has been least-square best fitted to the corresponding $A_0 - A_\infty$ data for the full range of spectra (solid blue line) and the $A_0 - A_\infty$ has been least square fitted to the corresponding $A_M - A_S$ data (solid green line), also for the full range of wavelengths used. The same applies to Fig. 13D, where no muscle sample is present. The fraction of BAPTA bound to Ca^{2+} (f) is given by the best-fit scaling factor relating $(A_0 - A_M) / (A_0 - A_\infty)$, which equals $(A_M - A_0) / (A_\infty - A_0)$ (Eq. 6). Correspondingly, the best-fit scaling factor of $(S_0 - S_M) / (S_0 - S_\infty)$ (or $(S_M - S_0) / (S_\infty - S_0)$) gives $f_{background}$ (Eq. 10).

3 Calcium content of the heart

Calcium content of mice left ventricle was measured. From each heart excised, two samples of the left ventricle were measured and their $[Ca_T]_{WM}$ values averaged. We determined $[Ca_T]_{WM}$ to be 2.55 mmol/kg wet muscle (n = 6, SEM = 0.21).

As mentioned in the materials and methods section, an attempt was made to wash out the extracellular calcium in order to measure the intracellular calcium and, like this, improve the accuracy of our determination. One samples from each heart was left for 30 min in a Ca-free, Na-free solution. The Na-free solution is aimed to stop the activity of the NCX. The measured $[Ca_T]$ was 1.27 mmol/kg wet muscle (n = 7, SEM = 0.05). Assuming all the calcium in the extracellular solution was removed and there was no loss of intracellular calcium, this result indicates that only half of $[Ca_T]$ in the heart solution is intracellular.

4 Effects of epinephrine and exercise on $[Ca_T]$

Table 2 shows a summary of the average $[Ca_T]$ values of the muscles studied obtained under the different conditions applied.

4.1 Samples collected for each condition

Left and right EDL, Sol, BCP, BR and the heart were collected from 6 mice/condition.

4.2 Administration of an epinephrine or saline injection

$[Ca_T]_{WM}$ values obtained from control mice, mice injected with epinephrine and mice injected with saline were compared. An epinephrine injection caused a $[Ca_T]_{WM}$ reduction in all the muscles studied, although, as detailed later, this reduction was not significant in all the cases. On the other hand, a saline injection also led to a decrease of the $[Ca_T]_{WM}$ in all the muscles studied, with the exception of the EDL (Fig 13A, Table 2).

Concerning the EDL, there is a statistically significant difference between the group injected with epinephrine and both the group injected with saline ($p<0.01$) and the control group ($p<0.01$), being the $[Ca_T]_{WM}$ values lower in the epinephrine group. There is no significant difference between the group injected with saline and the control group. For both the Sol

and the BR, both the epinephrine and the saline injections caused a statistically significant $[Ca_T]_{WM}$ reduction, compared to the control group ($p<0.01$ in both cases). However, there is not a significant difference between the epinephrine and the saline groups. In the case of the BCP, no significant difference was found after neither of the two injections. In the heart, a saline injection caused a significant reduction, when compared to the control group ($p<0.01$), whereas, unexpectedly, no difference was found between the group injected with epinephrine and both the saline group and the control group (Table 3).

4.3 Administration of an epinephrine or a saline injection combined with the treadmill training

To determine the short-term effects of adrenergic stimulation when combined with exercise, $[Ca_T]_{WM}$ values obtained from the mice injected with epinephrine, the mice injected with saline, the mice injected with epinephrine and exercised, and the mice injected with saline and exercised were compared among each other. For all the muscles studies, the group injected with epinephrine and exercised showed a significant reduction of $[Ca_T]_{WM}$ when compared to the groups that were just injected with either epinephrine or saline (Fig 13B, Table 2). Regarding the group that was injected with saline and exercised, $[Ca_T]_{WM}$ values were always lower when compared to the groups that were just injected with either epinephrine or with saline, although this difference was less drastic and, in some cases, not significant (Fig 13B, Table 2).

Regarding the EDL, the fact of combining either an epinephrine or a saline injection with the treadmill training caused a statistically significant reduction of $[Ca_T]_{WM}$, when compared to the administration of the injections alone ($p<0.01$ in all the cases). In the soleus and the BCP, the combination of an epinephrine injection with the exercise reduced $[Ca_T]_{WM}$ significantly, when compared to the groups that were just injected with either epinephrine ($p<0.01$ in both cases) or saline ($p<0.05$ in the case of the soleus and $p<0.01$ in the case of the BCP). However, no difference was found between the groups injected with a saline solution and exercised and the groups that were just injected. Concerning the BR, the combination of an epinephrine injection with the exercise reduced $[Ca_T]_{WM}$ significantly when compared to the groups that were just injected with either epinephrine or saline ($p<0.01$ in both cases) and, contrary to other muscles, a significant reduction was also found between the group injected with saline and exercised and the group injected with saline ($p<0.05$). Interestingly, $[Ca_T]_{WM}$ values of the group injected with epinephrine and exercised were

significantly lower than those of the group injected with saline and exercised ($p<0.05$). Finally, for the heart, the same significant reduction of $[Ca_T]_{WM}$ was found between the group injected with epinephrine and exercised and the groups that were just injected with either epinephrine ($p<0.01$) or saline ($p<0.05$). However, in this case the group injected with saline and exercised showed significantly lower values than the group injected with epinephrine ($p<0.05$), although, interestingly, no difference was found with respect to the group that was just injected with saline (Table 4).

4.4 Treadmill training

To evaluate the effect of exercise on $[Ca_T]_{WM}$, we compared the results obtained from the control group and the group trained in the treadmill. Whereas no difference was found in most of the muscles studied we found a statistically significant increase of $[Ca_T]_{WM}$ in the EDL of the exercised group ($p<0.01$). As shown in Table 2, the mean $[Ca_T]_{WM}$ values are 2.91 mmoles/kg (S.E.M. = 0.11 mmoles/kg; N = 12) and 4.57 mmoles/kg (S.E.M. = 0.21 mmoles/kg; N=12) for the control and the exercised groups, respectively. This is an important result, covered further in the Discussion.

		EDL	Sol	BCP	BR	Heart
Control						
Mean mouse weight (g)	17.4					
Mean muscle weight (mg)		7.56	5.64	9.69	3.96	8.12
$[Ca_T]_{WM}$ range (mmol / kg wet muscle)		2.30 – 3.42	1.47 – 3.96	1.94 – 3.28	2.88 – 5.50	1.72 – 3.33
Mean $[Ca_T]_{WM}$ (mmol / kg wet muscle)		2.91	3.27	2.30	4.33	2.55
SEM		0.11	0.21	0.13	0.19	0.21
N		12	11	12	12	6
Epinephrine						
Mean mouse weight (g)	19.33					
Mean muscle weight (mg)		8.46	6.23	10.3	4.3	9.5
$[Ca_T]_{WM}$ range (mmol / kg wet muscle)		1.09 – 3.16	1.37 – 3.42	1.44 – 2.91	1.79 – 3.61	1.03 – 3.50
Mean $[Ca_T]_{WM}$ (mmol / kg wet muscle)		1.96	2.36	1.91	2.43	1.91
SEM		0.14	0.19	0.13	0.18	0.21
N		12	12	12	12	6

Saline

Mean mouse weight (g)	21.8					
Mean muscle weight (mg)		7.91	5.68	10.41	4.56	9.74
$[Ca_T]_{WM}$ range (mmol / kg wet muscle)		1.56 – 4.20	1.47 – 3.34	1.24 – 5.98	1.56 – 4.13	0.75 – 2.13
Mean $[Ca_T]_{WM}$ (mmol / kg wet muscle)		2.98	2.10	1.96	2.98	1.41
SEM		0.25	0.19	0.37	0.25	0.17
N		12	12	12	12	6

Epinephrine + Exercise

Mean mouse weight (g)	19.92					
Mean muscle weight (mg)		7.64	5.55	11.43	3.91	9.02
$[Ca_T]_{WM}$ range (mmol / kg wet muscle)		1.19 – 1.43	0.27 – 1.96	0.43 – 1.31	0.32 – 1.83	0.19 – 0.75
Mean $[Ca_T]_{WM}$ (mmol / kg wet muscle)		0.88	0.89	0.84	1.97	0.51
SEM		0.23	0.11	0.15	0.23	0.38
N		12	12	12	11	6

Saline + Exercise

Mean mouse weight (g)	17.97					
Mean muscle weight (mg)		7.68	5.31	9.7	3.66	7.60
$[Ca_T]_{WM}$ range (mmol / kg wet muscle)		0.26 – 1.81	0.30 – 5.11	0.68 – 3.02	0.92 – 3.70	0.66 – 1.87
Mean $[Ca_T]_{WM}$ (mmol / kg wet muscle)		1.08	1.88	1.20	0.94	1.14
SEM		0.11	0.15	0.08	0.11	0.10
N		11	12	10	10	6

Exercise

Mean mouse weight (g)	18.45					
Mean muscle weight (mg)		7.24	5.65	10.55	3.8	8.42
$[Ca_T]_{WM}$ range (mmol / kg wet muscle)		3.05 – 6.27	3.00 – 4.06	2.11 – 3.63	3.05 – 6.27	0.34 – 3.01
Mean $[Ca_T]_{WM}$ (mmol / kg wet muscle)		4.57	3.36	2.47	4.57	1.87
SEM		0.21	0.46	0.23	0.33	0.16
N		12	12	12	12	6

Table 2. Summary of the data obtained. The table shows muscle and mouse weight, ranges of $[Ca_T]_{WM}$ values, average $[Ca_T]_{WM}$ values as well as the SEM and the number of samples.

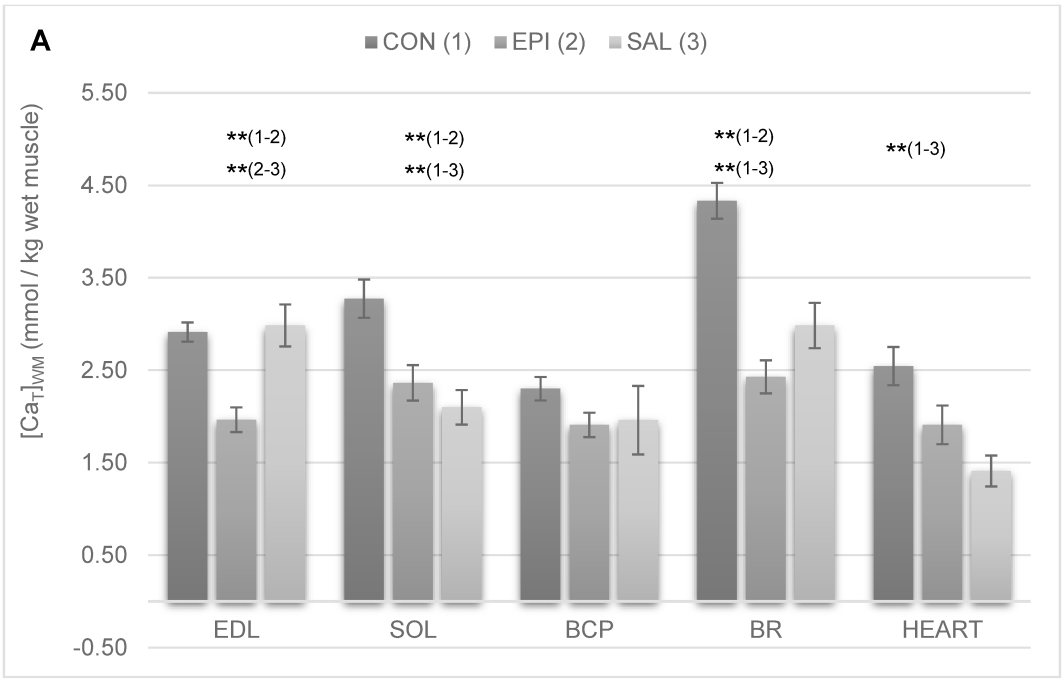
A
CON (1)
EPI (2)
SAL (3)
[Ca_T]_WM (mmol / kg wet muscle)
5.50
4.50
3.50
2.50
1.50
0.50
-0.50
**(1-2)
**(2-3)
**(1-2)
**(1-3)
**(1-2)
**(1-3)
**(1-3)
EDL
SOL
BCP
BR
HEART

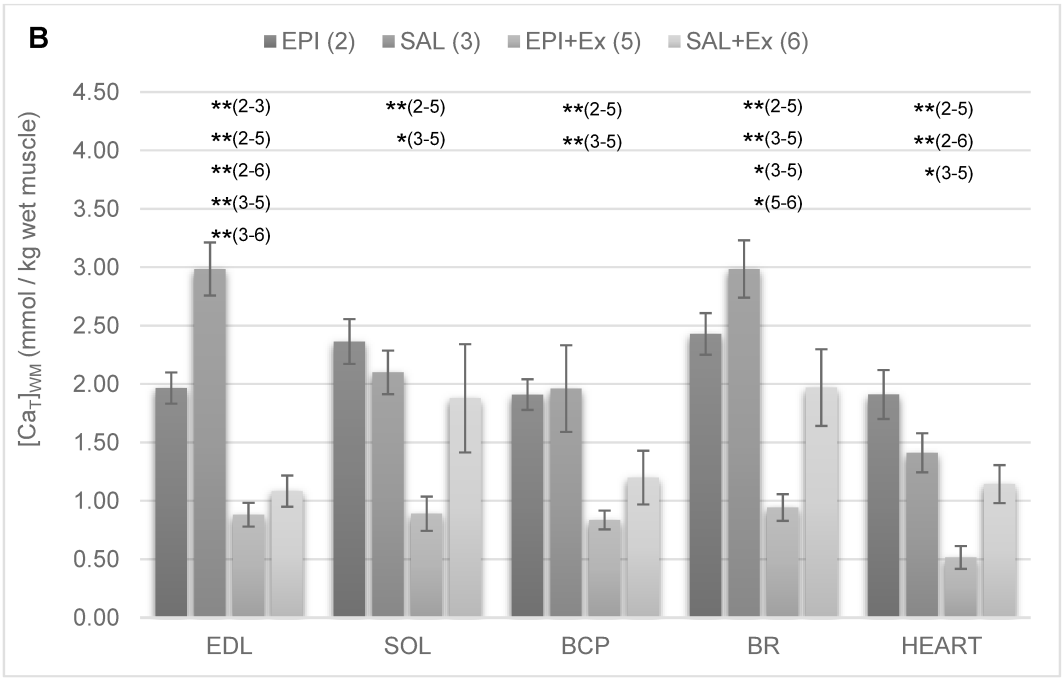
B
EPI (2)
SAL (3)
EPI+Ex (5)
SAL+Ex (6)
[Ca_T]_WM (mmol / kg wet muscle)
4.50
4.00
3.50
3.00
2.50
2.00
1.50
1.00
0.50
0.00
**(2-3)
**(2-5)
**(2-6)
**(3-5)
**(3-6)
**(2-5)
*(3-5)
**(2-5)
**(3-5)
**(2-5)
**(3-5)
*(3-5)
*(5-6)
**(2-5)
**(2-6)
*(3-5)
EDL
SOL
BCP
BR
HEART

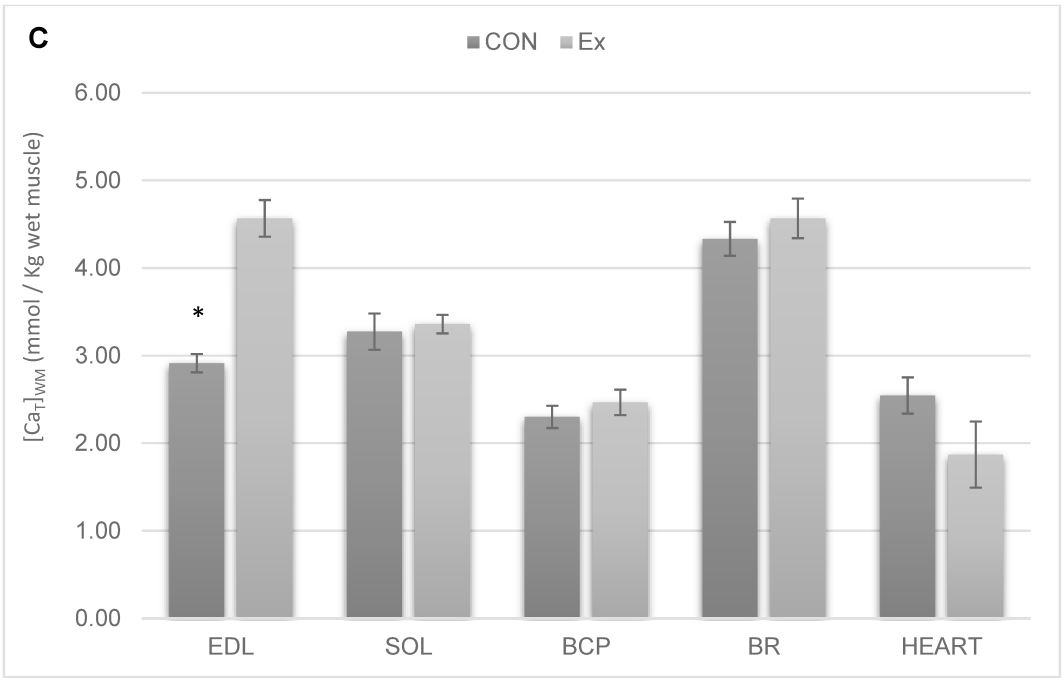

Figure 13. Calcium content ($[Ca_T]_{WM}$) of mice *extensor digitorum longus* (EDL), soleus (Sol), biceps (BCP), *brachioradialis* (BR) was calculated. 36 mice were assigned to one of the following groups: 1) control mice (CON), 2) mice injected with epinephrine (EPI), 3) mice injected with saline (SAL), 4) mice exercised in a treadmill (Ex), 5) mice injected with epinephrine and exercised in a treadmill (EPI+Ex), 6) mice injected with saline and exercised in a treadmill (SAL+Ex), and the $[Ca_T]_{WM}$ results compared. Fig. 13A shows the comparison between groups CON, EPI and SAL for each of the muscle types. Fig. 13B compares groups EPI, SAL, EPI+Ex and SAL+Ex for each of the muscle types. Fig. 13C shows the results of groups CON and Ex. Each pair of groups is compared. A p-value<0.05 indicates a statistically significant difference. A p-value<0.01 indicates a strong statistically significant difference. The numbers in brackets indicate between which groups that difference is found. These numbers are absent in the last graph since only two conditions are being compared.

CONTROL Vs EPINEPHRINE Vs SALINE			
		CON	**EPI**
EDL			
	EPI	p<0.01	-
	SAL	Not significant	p<0.01
Sol			
	EPI	p<0.01	-
	SAL	p<0.01	Not significant
BCP			
	EPI	Not significant	-
	SAL	Not significant	Not significant
BR			
	EPI	p<0.01	-
	SAL	p<0.01	Not significant
Heart			
	EPI	Not significant	-
	SAL	p<0.01	Not significant

Table 3. Statistical comparison of total calcium concentration in the muscle of mouse *extensor digitorum longus* (EDL), soleus (Sol), biceps (BCP), *brachioradialis* (BR) and heart in three different conditions: control mice (CON), mice injected with epinephrine (EPI) and mice injected with a saline solution (SAL). The difference among the treatments is considered very statistically significant when p<0.01 and statistically significant when p<0.05.

EPINEPHRINE Vs SALINE Vs EPINEPHRINE + EXERCISE Vs SALINE +EXERCISE				
		EPI	**SAL**	**EPI+Ex**
EDL				
	SAL	p<0.01	-	p<0.01
	EPI+Ex	p<0.01	p<0.01	-
	SAL+Ex	p<0.01	p<0.01	Not significant
Sol				
	Sal	Not significant	-	p<0.01
	EPI+Ex	p<0.01	p<0.01	-
	SAL+Ex	Not significant	Not significant	Not significant
BCP				
	SAL	Not significant	-	p<0.01
	EPI+Ex	p<0.01	p<0.01	-
	SAL+Ex	Not significant	Not significant	Not significant
BR				
	SAL	Not significant	-	p<0.01
	EPI+Ex	p<0.01	p<0.01	-
	SAL+Ex	Not significant	p<0.05	p<0.05
Heart				
	SAL	Not significant	-	p<0.05
	EPI+Ex	p<0.01	p<0.05	-
	SAL+Ex	p<0.05	Not significant	Not significant

Table 4. Statistical comparison of total calcium concentration in the muscle of mouse *extensor digitorum longus* (EDL), soleus (Sol), biceps (BCP), *brachioradialis* (BR) and heart in four different conditions: mice injected with epinephrine (EPI), mice injected with a saline solution (SAL), mice injected with epinephrine and that went under treadmill training (EPI+Ex), mice injected with a saline solution and that underwent treadmill training (SAL+Ex). The difference among the treatments is considered very statistically significant when p<0.01 and statistically significant when p<0.05.

DISCUSSION

1. Adaptation of the BAPTA method to the use of a plate reader for absorbance measurements

The main advantage that this modification of the BAPTA method has brought us is time economy. The use of the spectrophotometer, although adequate for this kind of measurement, allows the analysis of one sample at a time, an issue that has been overcome using the plate reader, where we can measure up to 47 samples at the same time. The substitution of the manual grinding by the automatic grinding was also a big step, since manual grinding is a hard process and time consuming. These two adaptations allowed us to analyze 540 samples in about two weeks, a process that would have taken several months with the use of the spectrophotometer.

During the development of the original BAPTA method, the authors made certain assumptions concerning BAPTA behavior. One of them, (Assumption 2 in Lamboley *et al.*, 2015) stated that the method works because elements other than calcium were either present in a much lower concentration in the solution than calcium or their binding affinity for BAPTA was much lower. Quian & Colvin suggested in 2015 that, although this assumption is true for most elements, such as Mg^{2+} and protons, it does not apply to zinc, since it is known that Zn^{2+} competes with calcium for several calcium-binding sites including those on BAPTA and EGTA (Quian & Colvin, 2015). As a result, the BAPTA method reports the sum of the concentrations of total calcium and total zinc in the tissue. [Zn]i is reported to be 100-fold less than resting cytosolic free calcium (Colvin, 2008). More importantly, using an adaptation of our BAPTA method, Quian & Colvin (2015) estimated that total Zn content was only about 15% of total calcium content. This adaptation involves the use of TPEN - a Zn^{2+} chelator with a higher affinity for Zn^{2+} compared to those for BAPTA and EGTA – in order to isolate the zinc and calcium components. This idea has been welcomed in our laboratory and the samples used in this study have also been analyzed including the TPEN, although the data are not shown in this document.

2. Calcium content of the heart

Calcium content measurements following the BAPTA method gave much higher values regarding [Ca_T] in the heart than those in the literature obtained by using isolated cardiomyocytes. One possible explanation is that the calcium measured comes from the extracellular space rather than the intracellular space. To address this issue and as explained earlier in this document, from each mouse used, one of the samples was left 30 min in 0Ca-0Na modified mammalian Ringer's solution whereas the rest were treated normally (see materials and methods). Indeed, the values obtained from the samples left in 0Ca-0Na show about a twofold decrease in $[Ca_T]_{WM}$ with respect to the others. This difference could indeed mean that there is an important extracellular component that needs to be considered.

There are other issues to consider regarding our estimate. As mentioned before, cells other than myocytes could also be a source of calcium. Something interesting to point out is that extracellular calcium and sodium wash out is not an instant process and the presence of sodium in the extracellular space before it has a chance to diffuse away still allows the loss of Ca^{2+} due to the activity of the NCX.

An issue that has also been under question is the composition of the tissue examined. Unlike isolated cardiomyocytes preparations, different types or tissue are present in our preparations. Assuming the extracellular space to be similar to that of the skeletal muscle, it represents 12.4% of the heart (Lamboley *et al*., 2015). Regarding the different types of cells that can be found, cardiomyocytes represent 75% of the tissue volume (Camelliti et al., 2005) and the 12.6% left corresponds to other kind of cells, specially, fibroblasts. Based on that, $[Ca_T]_{WM}$ is estimated taking into account three different components: the extracellular compartment, the myocytes and the cells other than myocytes. The following equation sums the contribution of each element in terms of fractions:

$$W_M\left[Ca_T\right]_{WM} = 0.124 \cdot W_M \cdot \left[Ca_T\right]_{EC} + 0.126 \cdot W_M\left[Ca_T\right]_{non\_myo} + 0.75 \cdot W_M\left[Ca_T\right]_{myo} \qquad (10)$$

where W_M is the weight of the muscle, $[Ca_T]_{WM}$ is the measured calcium concentration, $[Ca_T]_{EC}$ corresponds to the calcium concentration in the extracellular space, $[Ca_T]_{non\_myo}$

represents the calcium concentration of cells other than myocytes and $[Ca_T]_{myo}$ is the calcium concentration of the myocytes.

Assuming an extracellular calcium concentration of 1.8 mM, we propose two cases. In case 1, $[Ca_T]$ of cells other than myocytes equals 0. In case 2, we assume that the [Ca] of cell other than myocytes is the same as in cardiomyocytes. Using the value of 1.27 mmol/kg with extracellular calcium removed in the equation above, $[Ca_T]_{myo}$ is 1.69 (1.27 ÷ 0.75) and 1.50 (1.27 ÷ (0.126 + 0.75)) mmol/kg for case 1 and 2, respectively.

Estimates of the extracellular component are also of potential interest. With the value of 2.55 mmol/kg for $[Ca_T]_{WM}$, the above equation gives values for extracellular calcium, $[Ca_T]_{EC}$, of 10.3 ((2.55 – 0.75 * 1.69) ÷ 0.124) and ((2.55 – (0.75 + 0.126) * 1.50) ÷ 0.124) and 9.9 mmol/kg for cases 1 and 2, respectively. While we have no proof yet, we suspect that these high concentrations, near 10 mmol/kg, are due to a loss of intracellular calcium during the exposure to the 0Ca-0Na. If this was the case, the values above of 1.69 and 1.50 mmol/kg wet muscle weight underestimate $[Ca_T]_{myo}$. For simplicity with the further evaluations below, we use the average of these two estimates, 1.60 mmol/kg, for $[Ca_T]_{myo}$. Assuming a density of 1 kg per L, the corresponding value of $[Ca_T]_{myo}$ referred to myocyte volume is 2.13 mmol/L of myocyte (2.13 = 1.60 ÷0.75).

Calcium content in rat heart was reported to be 114 µmol/L cytosol (Bassani & Bers, 1995). In order to compare this value to ours, we used the following equation to express our data in the same units:

$$\left[Ca_T\right]_{ref\_to\_myo} = (1/0.7) \cdot \left[Ca_T\right]_{myo} \quad (11)$$

where $[Ca_T]_{ref\_to\_myo}$ refers to the concentration of total calcium referred to the cytoplasmic volume of the myocyte and 0.7 is a factor corresponding to the estimated fraction of muscle - cell volume occupied by cytosolic water rather than filaments and organelles.

Applying this conversion, we obtain a new value, $[Ca_T]_{Heart}$ = 3057 µmol/L cytosol (1000 x 2.14 ÷ 0.7). The ratio obtained comparing this value to those provided by Bers (1995) is 26.8 (3057 ÷114). As mentioned in the Introduction, we suspect this very large discrepancy to be a result of the methods followed by the authors who performed these measurements on isolated cardiomyocytes instead of an entire tissue. The implications of this results are quite strong. Measurement of calcium dynamics in the heart has been useful to study

several physiological processes and pathologies, as stated in the Introduction of this document. However, the cardiomyocyte preparation used to study cardiac pathophysiology appears to have [Ca_T] values much lower than the physiological level, probably owing to the loss of calcium during the Ca-free period of the protocol for preparing cardiomyocytes. Our results suggest that the field of EC-coupling in cardiac muscle needs to be reconsidered.

3. Effects of epinephrine and exercise on $[Ca_T]_{WM}$

3.1 Administration of an epinephrine or saline injection

It is agreed that several cell components are affected by adrenergic stimulation. β-adrenergic receptors (β-AR) (located on the sarcoplasmic membrane of muscle cells) are G-coupled receptors that respond to several catecholamines such as epinephrine (i.e., Strosberg, 1993). The binding of epinephrine to the β-AR causes an increase of cAMP production via adenylyl cyclases (AC). The main target for cAMP is protein kinase A (PKA), that phosphorylates the LTCC, the RyR, and PLB (Kubota *et al*., 2002; El-Armouche & Eschehagen, 2009). Phosphorylation of PLB relieves the inhibition of the SERCA pump, which enhances the return of calcium to the SR (El-Armouche & Eschenhagen, 2009). Because of this, a reduction of $[Ca_T]_{WM}$ in all muscles studied after an epinephrine injection has come as a surprise. One of the characteristics of the "fight or flight" response (mediated by the sympathetic nervous system through epinephrine and norepinephrine release) is a rapid decrease in diastolic [Ca^{2+}] in the cytosol in order to allow a rapid muscle relaxation (El-Armouche & Eschehagen, 2009). Most of this calcium is sequestered by the SR thanks to the activity of the SERCA pump. However, calcium can also be extruded towards the extracellular compartment thanks to the activity of different structures located in the sarcoplasmic membrane. Among them, the NCX is thought to be the main responsible. Some studies have reported an increase on the expression (i.e., Reinecke *et al.*, 1997) and activity (i.e., Stengl *et al*., 1997) of the NCX under α-adrenergic stimulation. Since the epinephrine (used in our experiments) is not a specific β-adrenergic agonist, one explanation to our results is that α-adrenergic stimulation might also be playing a role in intracellular calcium handling, enhancing the activity of the NCX. The measured $[Ca_T]_{WM}$ would be, then, a result of the counteracting effects of β-adrenergic stimulation, that would

increase $[Ca_T]_{WM}$ and α-adrenergic stimulation, that would increase the extrusion of calcium towards the extracellular milieu, with a higher contribution of the later.

Saline injections also gave some interesting results. Since the “fight or flight” response is a process triggered naturally when facing any kind of stressor, any stress caused on the mice (such as the state of stress caused by the injections themselves) is expected to trigger endogenous epinephrine and norepinephrine production, giving an effect similar to that caused by the epinephrine injections. The group of mice injected with saline allows us to see the extent of the effect of this endogenous production on our results. The significant decrease in $[Ca_T]_{WM}$ caused by saline injections in two of the skeletal muscles studied (Sol and BR) is indicative of a possible important role of endogenous adrenergic agonists.

Since α-adrenergic receptors represent less than 10% of the adrenergic receptors present in the heart (O’Conell *et al.*, 2014) and the skeletal muscle, it is more likely that the α-adrenergic stimulation has a more important role at a systems physiology level, for example in the control of vascular tone (i.e.,Nash, 1990) and salt retention. Niebylski *et al.* (2011) reported a diminished sodium excretion in stressed rats. According to the authors, these results can be explained, on the one hand, by an increase of aldosterone concentration, which would enhance salt retention by increasing the transportation and the novo synthesis of epithelial Na^+ channels, leading to an increase of intracellular $[Na^+]$ and, on the other hand, by an enhanced reabsorption of Na^+ due to the sympathetic stimulation and increased catecholamines levels associated to stressful situations. Vascular tone and salt retention might also play a role in calcium regulation in the muscle, although the extent of these effects cannot be assessed by the results obtained from our experiments.

3.2 Administration of an epinephrine or a saline injection combined with exercise

When an intraperitoneal injection of epinephrine was combined with exercise in the treadmill, the effects we saw when the intraperitoneal injection was applied alone were exacerbated. In the case of the administration of epinephrine without the exercise, $[Ca_T]_{WM}$ was reduced as a result of the α-adrenergic stimulation predominance over the β-adrenergic stimulation. On account of cells experiencing multiple action potentials during exercise, the cells will be more depolarized (on average) during exercise compared to the resting state, thereby enhancing the electrical driving force for calcium transport out of the cell. In addition, the chemical driving force is also enhanced owing to the enhanced sarcoplasmic $[Ca^{2+}]$

arising from SR Ca^{2+} release. In these conditions, the amount of calcium being extruded to the extracellular milieu by the NCX also increases leading to a smaller $[Ca_T]_{WM.}$ Once again, the activity of the NCX would also be enhanced by the large $[Ca^{2+}]$ in the sarcoplasm in exercise compared to control.

3.3 Treadmill training

This study was motivated by our hypothesis of a physiological mechanism by which the muscle would increase calcium content when force requirements increase. In regard to this hypothesis, the specific purpose of this study was to obtain a reproductible, short-term protocol for revealing this physiological mechanism so that it could be further investigated. According to our results, treadmill exercise increased $[Ca_T]_{WM}$ in mice EDL, with respect to our control group, but the mechanism by which the muscle builds up calcium is still not known. However, we now have reproductible conditions that can allow further investigation. In our laboratory, we are now interested in using differential mass spectrometry to reveal differences in protein expression and protein phosphorylation in exercised vs. rested EDL muscle.

One of our hypothesis involves an inward calcium flux different than the calcium current that goes through the LTCC. Several studies support the existence of non-selective cationic channels, the store-operated calcium channels (SOCs) and the stretch-activated channels (SACs), that can be activated, respectively, by depletion of internal calcium stores or by stretch, leading to an inward Ca^{2+} current (i. e., Allen *et al*., 2005).

Another possible explanation for the increase in $[Ca_T]$ in the EDL of the exercise group is that action potentials fire at a more rapid pace during exercise compared to the resting state, which results in an increase of Ca^{2+} current (ICa_L). This, together with the slow inactivation of the channels (that do not close completely in between action potentials, owing to this more rapid pace of firing), could lead to an intracellular calcium accumulation.

Although no theory can be ruled out based on our study, non-selective channels seem to be good candidates to look at when looking for contributors to this increase in $[Ca_T]_{WM.}$

Regarding the differences among the skeletal muscles studied, multiple reasons could explain the absence of a $[Ca_T]_{WM}$ increase, such as the type of exercise, that might require different degrees of involvement from each muscle or a different muscle composition (slow

vs fast twitch muscles). However, it is not possible to determine the exact cause explaining this variation.

As mentioned in the introduction of this document, we reported in 2015 a high $[Ca_T]_{WM}$ in the EDL and the heart of a group of mice that were agitated (stressed and exercising in their cage) with respect to a group of rested mice. In the present study, the results obtained after the application of our treadmill protocol agree with our previous results. However, no increase in calcium content of the heart was spotted. Once again, multiple explanations can apply, such as the difference on the age of the mice used for both experiments or the type of exercise suggested.

CONCLUSIONS

After dealing with several issues, mostly related to the $f_{background}$, the adaptation of the BAPTA method described by Lamboley *et al*. in 2015 proved to be both useful and faster than the original method, since it allows to measure up to 47 samples at the same time. The use of a mechanic grinder instead of a manual grinder was also an important contribution to the efficiency of the method. The analysis of the samples used in this study took around two weeks, whereas it would had taken several months were the original protocol used for the experiments. Further experiments are still needed, though, to handle the Zn^{2+} component, though this should only be on the order of 15% of the calcium component.

From $[Ca_T]_{WM}$ measurements preformed in the heart, we obtained values about 27 times higher than the values found in the literature, estimated from isolated cardiomyocytes rather than from entire tissue. Our hypothesis is that this big difference between our estimations and those previously reported by other authors, can be due to a problem related to the use of isolated cardiomyocytes. Further work needs to be done to address some issues related cardiac composition and the extracellular component,

Some conditions have been proven to act as regulators of calcium content both in skeletal and cardiac muscle. The role of adrenergic antagonists in $[Ca_T]_{WM}$ downregulation in all the tissues studied is probably a result of α - adrenergic stimulation dominating over β-adrenergic stimulation. The combination of adrenergic stimulation and exercise enhanced the calcium depletion of the cell started by the adrenergic stimulation alone, a situation where more calcium is being released to the cytosol from the SR, so more calcium can be extruded to the extracellular space. The $[Ca_T]_{WM}$ increase observed in the EDL after treadmill training might represent the calcium upregulation mechanism we are looking for, a situation where the muscle builds up intracellular calcium to satisfy force requirements. The channels responsible for calcium entry are yet to be identified.

REFERENCES

Allen, D. G.; Whithead, N. P.; Yeung, E. W. (2005) Mechanisms of stretch-induced muscle damage in normal and dystrophic muscle: role of ionic changes. *Journal of physiology. 567(3):723-735.*

Banerjee, I.; Fuseler, J. W; Price, R. L.; Borg, T. K.; Baudino, T. A. (2007) Determination of cell type and numbers during cardiac development in the neonatal and adult rat and mouse. *American journal of physiology – Heart and circulation physiology. H1883-H1891.*

Bassani, R. A.; Bers, D.M. (1995*)* Rate of diastolic calcium release from the sarcoplasmic reticulum of intact rabbit and rat ventricular myocytes. *Biophysics Journal. 68:2015–2022.*

Belcastro, A. N. (1993) Skeletal muscle calcium-activated neutral protease (calpain) with exercise. *Journal of Applied Physiology. 74(3):1381-1386.*

Bers, D. M (2002) Cardiac excitation – contraction coupling. *Nature, 415(6868):198-205.*

Bers, D. M.; Eisner, D. A.; Valdivia, H. H. (2003) SR Ca^{2+} and heart failure: roles of diastolic leak and Ca^{2+} transport. *Circulation Research, 93(6):487-490.*

Betts, J. G.; Desaix, P.; Johnson, E.; Johnson, J. E.; Korol, O.; Kruse, D.; Poe, B.; Wise, J. A.; Womble, M.; Young, K. A. (2013) *Anatomy and physiology*. Houston, TX: OpenStax CNX. Retrieved from: https://openstax.org/details/anatomy-and-physiology.

Calderon, J. C.; Bolaños, P.; Caputo, C. (2014) The excitation – contraction coupling mechanism in skeletal muscle. *Biophysics. Review. 6:133-160.*

Camelliti, P.; Borg, T.K.; Kohl, P. (2005) Structural and functional characterisation of cardiac fibroblasts. *Cardiovascular Research. 65(1):40-45.*

Colvin, R.A., A.I. Bush, I. Volitakis, C.P. Fontaine, D. Thomas, K. Kikuchi, and W.R. Holmes. 2008. Insights into Zn2+ homeostasis in neurons from experimental and modeling studies. *American journal of physiology - cell physiology. 294:C726–C742.*

Diaz, M. E.; Graham, H. K.; O'Neill, S. C.; Trafford, A. W; Eisner, D. A. (2005) The control of SR Ca content in cardiac muscle. *Cell Calcium. 38:391-396.*

Eisner, D. A.; Caldwell, J. L.; Kistamas, K.; Trafford, A. W. (2017) Excitation – contraction coupling in the heart. *Circulation Research. 121:181-195.*

El-Armouche, A.; Eschenhagen, T. (2009) β-Adrenergic stimulation and myocardial function in the failing heart. *Heart Fail Review. 14:225-241.*

Franzini-Armstrong, C.; Jorgensen, A. D. (1994) Structure and development of excitation - contraction coupling units in skeletal muscle. *Annual Review Physiology. 56:509–534.*

Fraysse, B.; Liantonio, A.; Cetrone, M.; Burdi, R.; Pierno, S.; Frigeri, A.; Pisoni, M.; Camerino, C.; De Luca, A. (2004) The alteration of calcium homeostasis in adult dystrophic mdx muscle fibers is worsened by a chronic exercise in vivo. *Neurobiology of disease. 17(2):144-154.*

Gilchrist, J. S.; Wang, KK, Katz S, Belcastro AN. (1992) Calcium-activated neutral protease effects upon skeletal muscle sarcoplasmic reticulum protein structure and calcium release. *Journal of biological chemistry*. *267:20857–20865.*

Grabarek, Z.; Tao, T.; Gergely, J. (1992) Molecular mechanism of troponin – C function. *Journal of Muscle Research & Cell Motility*. *13:383-393.*

Hasenfuss, G. (1988) Alterations of calcium-regulatory proteins in heart failure. *Cardiovasc Research. 37(2):279-89.*

Hobai, I. A.; O'Rourke, B. (2001) Decreased sarcoplasmic reticulum calcium content is responsible for defective excitation – contraction coupling in canine heart failure. *Circulation Research. 103(11):1577-1584.*

Kirbi, A. C.; Lindey, B. D. (1981) Calcium content of rat fast and slow muscle after denervation. *Comparative biochemistry and physiology – Part A: physiology. 70(4):583-586.*

Kirbi, A. C.; Lindey, B.D.; Picken, J. R. (1975) Calcium content and exchange in frog skeletal muscle. *Journal of physiology. 253(1):37-52.*

Kubota, I.; Tomoike, H.; Xinquiang, H.; Sakurai, K.; Endoh, M. (2002) The Na^{+}/Ca^{2+} exchanger contributes to β-adrenoceptor mediated positive inotropy in the mouse heart. *Japanese Heart Journal. 43(4):399-407.*

Lamboley, C.; Kake–Guena, S. A.; Touré, F.; Hébert, C.; Yaddaden, L.; Nadeau, S.; Bouchard, P.; Wei-LaPierre, L.; Lainé, J.; Rousseau, E. C.; Frenette, J.; Protasi, F.; Dirksen, R. T.; Pape, P. C. (2015) New method for determining total calcium in tissue applied to skeletal muscle with and without calsequestrin. *Journal of general physiology. 145(2):127-153.*

Landstrom, A. P.; Beavers, D. L.; Wehrens, X. H. T. (2014) The junctophilin family of proteins: from bench to bedside. *Trends in molecular medicine. 20(6):353-362.*

Laustiola K, Uusitalo A, Koivula T, et al. (1983) Divergent effects of atenolol, practolol and propranolol on the peripheral metabolic changes induced by dynamic exercise in healthy men. *European Journal of Clinical Pharmacology*. *25(3):293-297.*

Lindner, M.; Erdmann, E.; Beuckelmann, D. J. (1998) Calcium content of the sarcoplasmic reticulum in isolated ventricular myocytes from patients with terminal heart failure. *Journal of Molecular Cell Cardiology. 30:743–749.*

Mazala, D. A.; Grange, R. W.; Chin. E. R. (2015) The role of proteases in excitation-contraction coupling failure in muscular dystrophy. *American Journal of Physiology. 308(1):C33-C40.*

McDonell, A. F. & Pape, P. C. (2015) The concentration of total calcium in fast twitch and heart muscles from mice in an agitated and active state is almost two-fold greater than those from resting mice. *Biophysical Journal Vol. 110, Issue 3.* 60th Annual Meeting of the Biophysical Society, Los Angeles, California, United States (99a). *Abstract*.

Meyer, M.; Schillinger, W.; Pieske, B.; Holubarsch, C.; Heilmann, C.; Posival, H.; Kuwajima, G.; Mikoshiba, K.; Just, H.; Hassenfuss, G. (1995) Alterations of sarcoplasmic reticulum proteins in failing human dilated cardiomyopathy. *Circulation. 92:778 – 784.*

Murphy, R. M.; Dutka, T. L.; Horvath, D.; Bell, J. R.; Delbridge, L. M.; Lamb, G. D. (2013) Ca^{2+} - dependent proteolysis of junctophilin-1 and junctophilin-2 in skeletal and cardiac muscle. *Journal of physiology. 591: 719–729.*

Nash, D. T. (1990) Alpha-adrenergic blockers: mechanism of action, blood pressure control, and effects on lipoprotein metabolism. *Clinical cardiology. 13: 764-772.*

Neef, S.; Maier, L. S. (2013) Novel aspects of excitation – contraction coupling in heart failure. *Basic Research Cardiology. 108(4):360-371.*

Niebylski, A.; Boccolini, A.; BEnsi, N.; Binotti, S.; Hansen, C.; Yaciuk, R.; Gauna, H. (2011) Neuroendocrine changes and natriuresis in response to socil stress in rats. *Stress and Health. 28:179-185.*

O'Conell, T. D.; Jensen, B. C.; Baker, A. J., Simpson, P. C. (2014) Cardiac $alpha_1$-adrenergic receptors: novel aspects of expression, signaling mechanisms, physiologic function and clinical importance. *Pharmacological reviews. 66(1):308-333.*

Pape, P.C.; Carrier, N. (2002) Calcium release and intramembranous change movement in frog skeletal muscle fibers with reduced (<250 µM) calcium content. *Journal of physiology. 539:253-266.*

Periasamy, M.; Kalyanasundaram, A. (2007) Serca pump isoforms: their role in calcium transport and disease. *Muscle & Nerve. 35(4):430-42.*

Peterson, B. Z.; DeMaria, C.; Yue, D. (1999) Calmodulin Is the Ca^{2+} Sensor for Ca^{2+}-Dependent Inactivation of L-Type Calcium Channels. *Neuron. 22(3):549-558.*

Piacentino, V III.; Weber, C. R.; Chen, X.; Weisser-Thomas, J.; Margulies, K. B.; Bers, D. M. Houser, S. R. (2003) Cellular basis of abnormal calcium transients of failing human ventricular myocytes. *Circulation Research, 92:651–658.*

Porter, K.; Palade, G. (1957) Studies on endoplasmic reticulum. III. Its form and distribution in striated muscle cells. *Journal of Biophysics Biochemical Cytology. 3(2):269-300.*

Posterino, G. S.; Lamb, G. D. (2003) Effect of sarcoplasmic reticulum Ca2+ content on action potential-induced Ca2+ release in rat skeletal muscle fibres. *Journal of physiology. 551(1):219–237.*

Powers, S. K.; Jackson, M. J. (2008) Exercise-induced oxidative stress: cellular mechanisms and impact on muscle force production. *Physiology Review. 88:1243-1276.*

Protasi, F. (2002) Structural interaction between RyRs and DHPRs in calcium release units of cardiac and skeletal muscle cells. *Frontiers bioscience. 7.*

Quian, C.; Colvin, R. A. (2015) Zinc flexes its muscle: Correcting a novel analysis of calcium for zinc interference uncovers a method to measure zinc. *Journal of general physiology. 147(1): 95- 102.*

Reinecke, H.; Vetter, R.; Drexler, H. (1997) Effects of alpha-adrenergic stimulation on the sarcolemmal NCX in adult rat ventricular cardiomyocytes. *Cardiovascular Research. 36(2):216-222.*

Schneider, M. F.; Chandler, W. K. (1993) Voltage dependent charge movement of skeletal muscle: a possible step in excitation – contraction coupling. *Nature. 242(5395):244-6.*

Schwinger, R. H.; Münch, G.; Bölck, B.; Karczewski, P.; Krause, E. G.; Erdmann, E. (1999) Reduced Ca^{2+}-sensitivity of $SERCA_2$a in failing human myocardium due to reduced serin-16-phospholamban phosphorylation. *Molecular Cell Cardiology. 31(3):479-491.*

Singh, R.B.; Chohan, P. K.; Dhalla, N. S.; Netticadan, T. (2004) The sarcoplasmic reticulum proteins are targets for calpain action in the ischemic-reperfused heart. *Journal of molecular and cellular cardiology. 37:101-110.*

Stengl, M.; Mubagwa, K.; Carmeliet, E.; Flameng, W. (1998) Phenylephrine-indiced stimulation of Na+/Ca2+ exchange in rat ventricular myocytes*. Cardiovascular research. 38:703-710.*

Strosberg, A. D. (1993) Structure, function and regulation of adrenergic receptors. *Protein Science. 2:1198-1209.*

Tortora, G. and Derrickson, B. (2011). *Principles of anatomy & physiology*. 13th ed. John Wiley & Sons, pp.523-571.

Yoshida, M.; Yonetari, A.; Shirasaki, T.; Wada, K. (2006) Dietary supplementation prevents muscle necrosis in a mouse model of Duchenne muscle dystrophy. *American Journal of Physiology. 290(2): R449 - R455.*

Zouhal, H.; Jacob, C.; Delamarche, P.; Gratas-Delamarche, A. (2008) Catecholamines and the effects of exercise, training and gender. *Sports Medicine. 38(5):401-423.*